# Resource Assessment of Undiscovered Seafloor Massive Sulfide Deposits on an Arctic Mid-Ocean Ridge: Application of grade and tonnage models

**Cyril Juliani, Steinar Løve Ellefmo**

Norwegian University of Science and Technology (NTNU), Department of Geoscience and Petroleum, Sem Sælandsvei 1, 7491, Trondheim, Norway

Corresponding author: Cyril Juliani

Corresponding e-mails: cyril.juliani@ntnu.no, steinar.ellefmo@ntnu.no

Phone number: +47 73 59 48 56

**Keywords** seafloor massive sulfide, mid-ocean ridge, resource assessment, grade, tonnage

**Abstract**

Norway has started ongoing initiatives related to deep sea mining. These include the evaluation of mineral resources within its sovereign territorial waters on the deep ocean floor of the Arctic region, i.e. the Mohns Ridge (71-73°N). Among the variety of possible seabed resources, seafloor massive sulfides (SMS) attract particular interest. Owing to the significant development potential and the general lack of knowledge of the SMS deposits, the present study aims at assessing mineral resources (i.e., Cu, Zn, Au and Ag) from a number of undiscovered sulfide deposits with the help of a revised model for mafic-hosted volcanogenic massive sulfide (VMS) deposits that adequately corresponds to geological settings of slow-spreading ridges. Application of the model requires a priori knowledge of the seafloor terrain to depict favorable geologic environments for the occurrence of SMS deposits. In such context, estimates are conducted for the easily accessible volcanically active parts of the ridge where 11 undiscovered deposits are expected. In these areas, total metal endowments are calculated to be on average 447,000 tonnes using a Monte Carlo simulation that combines the probabilistic estimates of number of undiscovered deposits with the grade and tonnage models. Estimates of in-place metal resources are generated in cumulative distribution form to present expected amount of undiscovered metals at 90% confidence intervals.

## 1. Introduction

Over the past decade, there has been a growing commercial interest in deep-sea minerals (e.g., European Commission, 2015). These minerals come in a variety of forms, such as seafloor massive sulfides (SMS) (Hannington et al., 2010; Beaulieu et al., 2013) which are expected to contribute to the supply of precious and base metals (e.g., Cu, Zn, Au, and Ag). Initial assessments of seabed metal accumulations are part of national strategies to support the activities aimed at increasing the knowledge on the abundance and characteristics of the deposits. In this context, the Norwegian Research Council has funded a project to investigate exploitation technologies relevant to potential deposits off the country's coast along a large part of the Arctic Mid-Ocean Ridges (AMOR) located inside the Norwegian jurisdiction. Specifically, the Mohns Ridge has become an important subject of investigation where a few identified SMS occurrences occur in various localities (Pedersen et al., 2010). Current analysis of resource potential along this ridge (Juliani and Ellefmo, 2018) established that several mineral deposits (11 expected in neo-volcanic zones) remain to be found. However, the uncertainty about their tonnages and grades is largely due to the lack of knowledge about SMS orebodies. Part of current uncertainties may be addressed if quantitative analyses integrate the land-based volcanogenic massive sulfides (VMS) which are generally considered as fossil analogues of hydrothermal vents recognized in both oceanic spreading ridge and arc environments (Galley et al., 2007). In such cases, mineral resource assessments can be made possible given our geological understanding of VMS characteristics (e.g., grade, size, host-rock and tectonic setting; Galley et al., 2007).

Estimating how much mineral resource is left addresses efforts in making precise modeling of mineral potential within geologically prospective areas. By its nature, such modeling reflects a great deal of uncertainty because the formation of natural minerals is complex (geologic factor) and because subjective awareness accounts for a large part in the prediction process (human factor). To some extent, uncertainties can be compensated by justifying quantitatively estimates in probabilistic terms. Probabilistic assessment of the presence and value of undiscovered deposits can be done with the help of compiled information on known deposits and examinations of associated geological provinces. Ideally, this process should rely on analogies where similar well-explored geologic settings and grades and tonnages of well-explored deposits are indicative of the quality and size of undiscovered deposits (Singer and Menzie, 2010). When available, geoscience information about analogue deposits (e.g., ore distribution, abundance and quality) can be integrated into a system (deposit model) that serves as an estimation guide. According to Singer and Menzie (2010), a deposit model allows to differentiate geologic settings among the deposit types studied and depict specific grade-tonnage-density distributions. In this regard, a well-established method to make estimates of undiscovered resources based on deposit models is the three-part form of quantitative assessment provided by Singer (1993) and Singer and Menzie (2010). In practice, a certain type of deposit is considered, and prospective areas are delineated according to the type(s) of deposit(s) permitted by the geology. Amounts of total metals in these areas are further assessed given grade and tonnage models, and the number of undiscovered deposits estimated.

Descriptive statistics of worldwide deposit data are typically computed to conceptualize and construct deposit models (Singer and Menzie, 2010). Even though the essential attributes of SMS deposits are still incomplete for determining related mineralization extent, and thus economic potential, they provide bases to emphasize the complex interplay of different ore-forming processes in a variety of geological environments (Fouquet et al., 2010). Diverse mafic-hosted hydrothermal deposits have previously been described along the Mid-Atlantic Ridge, such as the TAG (26°30'N; Hannington et al., 1991; Rona et al., 1993; Humphris and Cann, 2000; Rona, 2005), Snakepit (23°37'N; Hannington et al., 1991; Fouquet et al., 1993; Krasnov et al., 1995) and Broken Spur (29°10′N; Murton et al., 1994; Duckworth, 1995), and related information on ore textures and grade distribution (e.g., Humphris et al., 1995; Hannington et al., 1998), alteration types (e.g., Honnorez et al., 1998), age range (e.g., Lalou et al., 1995; Cherkashov et al., 2016) and deposit sizes (e.g., Hannington et al., 1998; 2010), which provide important insights on ore-forming processes that have practical applications for developing mineral exploration strategies. In this study, SMS deposits are evaluated using grade-tonnage models within neo-volcanic terrains along the valley floors of an ultraslow-spreading ridge. The deposits in question are considered hosted in volcanic substratum and to consist of different proportions of copper- and zinc-rich minerals, with precious metals (e.g., gold and silver) being present in lesser quantity as byproducts. Because VMS deposits represent fossil analogues of active hydrothermal vents, particular attention will be addressed to integrate the characteristics of well-explored VMS deposits for which depositional environments share similar characteristics with modern occurrences. Related knowledge on deposit sizes and commodities of economic interest (i.e., Cu, Zn, Au and Ag) will be aggregated, analyzed and compared with modern SMS deposits, and thereafter used to establish grade and tonnages models. These models will act as guidelines to estimate frequency distributions of metal amounts along the Mohns Ridge with the help of conventional Monte Carlo procedures.

## 2. Study area

The Mohns Ridge is an ultra-slow spreading mid-ocean ridge (MOR) that can be described as a deep rifted axial zone with a slow spreading rate (15 mm/yr; Vogt, 1986). An analysis of the ridge was made possible in this study after a successful multibeam data collection by the Norwegian Petroleum Directorate (NPD) in collaboration with the Geological Institute of the Russian Academy of Sciences (GIN RAS). The ridge trend analyzed is oriented approximately N045° and extends for about 550 km along its axis within the Norwegian-Greenland Sea (Fig.1). The axial valley is associated with significant isolated neo-volcanic zones recognizable from their hummocky-type terrain and associated volcanic edifices (e.g. flat-topped volcanoes, conic or dome structures and eruptive fissures). The volcanic areas sometimes appear in the form of topographic highs or axial volcanic ridges (AVRs), separated by deep basins and generally marked by morphostructures (e.g., dome-shaped axial volcanic ridges, grabens, horsts and tilted blocks; Géli et al., 1994; Dauteuil and Brun, 1996) describing the interplay between magmatic supply variations and tectonism. The central AVRs often split with large ongoing fault offsets transporting pieces of crust onto the ridge flanks during amagmatic periods when tectonism predominates, as usually observed for volcanic ridges with non-steady state evolution (Kappel and Ryan, 1986; Pezard et al., 1992). These magmato-tectonic cycles presumably participate in the development of abyssal hills as crust moves away from the ridge axis through faulting occurring at the median rift (e.g., Parsons and Thompson, 1993; MacDonald et al., 1996). Because the rift is tectonically dynamic, it consists of numerous faulting features, among which typical bounding faults operating at variable extents (Dauteuil and Brun, 1996; Bruvoll et al., 2009) and allowing to depict the ridge width and respective valley floor (see details in Juliani and Ellefmo, 2018). Both neo-volcanic zones and the ridge valley trend were delimited for constraining areas permissive for the occurrence of SMS deposits.

## 3. Data

Since few seabed ore deposits have been drilled so far (e.g., Humphris et al., 1995; Zierenberg et al., 1998; Lipton et al., 2012), little is known about the interior of their orebodies, which makes the estimates of resource potential rather uncertain. Land-based VMS occurrences are reasonable alternatives for reducing assessment uncertainties because their comparison with modern SMS features important similarities and differences in their distribution, sizes, and bulk compositions (Franklin et al., 2005; Hannington et al., 2005). Ophiolite-hosted massive sulfide deposits are commonly preserved in extrusive lava units (Hannington et al., 1998; Galley and Koski, 1999), but related ophiolites often do not possess all the characteristics of the slow-spreading ridges. Nevertheless, characteristic features (e.g., host lithology, alteration and mineralogy and tectonic setting) are documented to compare well with modern deposits generated in the volcanically active parts of MORs. Compiling of such data serves as bases for determining the size, grade, and distribution of undiscovered deposits given the general principles of the three-part mineral assessment practice (Singer and Menzie, 2010).

Among the hundreds of known ophiolites, at least 25 complexes exhibit massive sulfide deposits (Galley and Koski, 1999) of which numerous sulfide depositions are presently located within e.g., the Troodos and Semail ophiolites along the Tethyan suture zones (Adamides, 1980; Alabaster et al., 1980). Related VMS deposits generally consist of conformable, massive body of sulfides characterized by Cu and Cu-Zn ores and a peculiar set of sulfide minerals i.e., pyrite + chalcopyrite + sphalerite ± marcasite ± pyrrhotite, that distinguish them into an independent Cyprus type (Franklin et al., 1981; 2005; Barrie and Hannington, 1999). Cyprus-type deposits were deduced in a given geologic environment, dominantly mafic volcanic rocks, that may be associated with gabbro, diabase, and ultramafic rocks of an ophiolite sequence; such features being characteristics of e.g., the Troodos (Gass, 1968; Moores and Vine, 1971), Semail (Alabaster et al., 1982; Lippard et al., 1986; Ernewein et al., 1988) and Mirdita ophiolites (Shallo, 1991; 1994; Beccaluva et al., 1994; Bortolotti et al., 1996). Mosier et al. (2009) improved this analogy by subdividing the deposit type into (i) mafic in a primitive oceanic back-arc and (ii) mafic in a mid-oceanic ridge. For both types, associated grade and tonnage models were developed upon 174 completely drilled mafic-hosted sulfide deposits for which average grades of valuable metals (Cu, Zn, Au and Ag) and tonnages are based on the total production, reserves, and resources at the lowest available cutoff grade (Mosier et al., 2009).

Based on lithostratigraphic studies, several Cyprus-type VMS occurrences such as those found in the above-mentioned ophiolites may be close analogues to those of the present-day hydrothermal systems of sediment-starved MORs (e.g., the TAG mound-stockwork complex; Hannington et al., 1998; Galley and Koski, 1999; Galley et al., 2007). These analogues generally have a vertical zonation of mineralization styles within a host-rock, where an apparent pyritic massive lens grades down into semi-massive, brecciated, or disseminated pyrites accompanied by minor base metal sulfides (e.g., chalcopyrite, sphalerite and pyrrhotite; Franklin et al., 1981). Underneath, pyritesilica breccias supplant a quartz-pyrite stockwork in relation to a chlorite-silica alteration pipe (Hannington et al., 1998); although the stockwork may or may not be present. Such characteristics in VMS deposits might be expected in modern sulfide mounds, but at variable extents since the latter are still forming and may differ in bulk mineralogy (e.g., anhydrite is absent in Troodos VMS deposits, but present in the TAG sulfide mound; Hannington et al., 1998).

Geochemical data for SMS occurrences, almost always inferred for samples taken from the surfaces of the deposits, were considered in this study for the number of vent sites (either active or inactive), while VMS deposits were chosen on the basis that mineralization developed Cu or Cu-Zn ores in close association with volcanics in ophiolite sequences (mid-ocean or back-arc spreading setting). For the latter, quantitative data on mineralized zones are generally confirmed from drill cores and mining production; no distinction is made between production and reserve data though. Mineralizations in association with slow-spreading ridge-derived ophiolites (i.e., Troodos and Mirdita; Moores and Vine, 1971; Hurst et al., 1987, 1994; Dilek and Eddy, 1992; Varga et al., 1999; Nicolas et al., 1999; Tremblay et al., 2009; Robertson et al., 2012) were preferred for the tonnage model. The full data sets are provided as a digital supplement to this paper in Supplementary Tables 1, 2 and 3.

## 4. Model setup

### 4.1. Permissive tracts and number of undiscovered deposits

Estimating how many SMS deposits remain to be found is, however, a difficult exercise since explorative activities have up to now concentrated essentially on active vent fields (e.g., Hannington et al., 2011), while there exists a potential for large numbers of inactive unknown sites with relatively uncertain spatial distribution. Few SMS occurrences, exemplified by the Loki's Castle vent field and Copper Hill, have been found along the Mohns Ridge (Pedersen et al., 2010). However, Juliani and Ellefmo (2018) estimated 11 expected undiscovered deposits within the neo-volcanic terrains along the valley floor of this ridge (i.e., over 2922 km2 or 55% of the valley floor), based on (1) the assumption that volcanic terrains are geologically favorable to the occurrence of SMS deposits (permissive tracts) and (2) a regressive law, developed after the analysis of several deposit types from worldwide explored permissive tracts, evidencing a strong correlation between deposit size, area permissive, and deposit density over different prediction levels (10th, 50th and 90th percentiles) (Singer and Kouda, 2011):

$$R_{50} = 4.2096 - 0.4987\ log_{10}area - 0.2252\ log_{10}size \quad (1)$$

$$L_{90}, U_{10} = R_{50} \pm t\ S_{y|s,a} \sqrt{\left(\frac{1 + 1/n + (3.175 - log_{10}\ area)^2(-0.3292 - log_{10}\ size)^2}{(n-1)S_sS_a}\right)} \quad (2)$$

where $R_{50}$ corresponds to the 50th percentile in the estimates of deposit density (deposit per 100,000 km2), $L_{90}$ and $U_{10}$ represent the 90th and 10th percentiles respectively for the density of deposits, t is the Student's t parameter, $S_{y|s,a}$ is the standard deviation of logarithmic values of deposit density given permissive area and deposit size, n is the number of permissive tracts studied worldwide, 3.175 is the mean logarithmic values of permissive tract area in square kilometers,-0.3292 is mean of logarithmic values of deposit tonnage in millions on metric tons in control tracts, 2.615 is the standard deviation of log-transformed deposit tonnages in permissive tracts, and 1.188 is standard deviation of logarithmic values of area of permissive tracts.

As the estimates from the equations (1) and (2) are initially re-scaled for 100,000 km2, densities are thus adjusted for the size of the tracts by multiplying them with the factor permissive area / 100,000 km2. Estimates on the number of deposits can then be calculated at the three different percent levels, using the estimated values as exponents to the power of 10:

$$N = (permissive\ area/100{,}000) * 10^{\log_{10}(Density)} \quad (3)$$

Because the estimates made by Juliani and Ellefmo (2018) are relatively restricted to zones of observable volcanic accretions, similar regressive analyses were also conducted in this study over the entire ridge valley area (i.e., over 5065 km2 of seafloor) to depict what remains to be found over the full ridge length if magmatic expansion is hypothesized to be the main driver for spreading processes throughout the Mohns Ridge. Results are shown in Table 1.

### 4.2. Grade and tonnages models

Grade and tonnages models, such as those from Cox and Singer (1986), are reasonable solutions to represent the likelihood of resource potential at the regional scale. Such prediction takes the form of frequency distributions of size and average grades of well explored deposits (Singer, 1993). The models rely on lognormally distributed deposit size and commodity grades, where the logarithms of tonnage and grade of deposits are plotted versus the calculated proportion of the deposits. Grade-tonnage data distribution commonly show a positive skewness, and the mean and standard deviation of those data allow to fit a curve. To develop the distribution models, a compilation of quantitative historic information about the deposit type being studied is required. Ideally, such information is retrieved from well-explored deposits located in settings of geologic interest. The data in question generally include average grades of each metal of economic interest and the associated tonnage based on the total production, reserves and resource at the lowest possible cutoff grade (Singer and Menzie, 2010). It is possible to observe correlations between tonnage and grade (e.g., with Zn in mafic VMS subtype, i.e. r = -0.40; Mosier et al., 2009) and between grades of two commodities (e.g., Zn and Au with Ag in the same VMS subtype, i.e. r = 0.48 and 0.40 respectively; Mosier et al., 2009). Such relationships would be viable if the considered commodities are associated with the same mineral, but these tend to be rather complex to determine between deposits (Singer and Menzie, 2010) and in such cases, correlations are made statistically credible only to some degree. For these reasons, grades and tonnages are assumed to be statistically independent in this study.

### 4.3. Metal endowment

Metal endowment of undiscovered resources has important implications for economic estimates of what is recoverable. An expected quantity of metal contained within the evaluated areas can be estimated by combining distributions of number of deposits, tonnages, and grades (Singer and Menzie, 2010). A Monte Carlo simulation builds up an estimate of the probability distribution for recoverable resources by repeated random sampling of individual distributions of number of deposits, tonnages, and grades. Technically, a random number of deposits is routinely sampled given a number of cycles (10,000 in this study) pre-defined for the simulation. For each selected deposit(s) in a cycle, the simulator randomly samples a tonnage value that will be multiplied by a random grade of all possible commodities (i.e., Cu, Zn, Au and Ag) evaluated. After multiplying, the resulting amounts of each metal in each of the simulated deposit(s) for a given cycle are added, and the metals are summed for the total permissive area studied. The simulation finally outputs cumulative distributions of in-situ metals (in million tonnes). The results are given in probabilistic terms with the aim of reducing and quantifying uncertainties existing for undiscovered metal resources at different prediction levels such as the P10, i.e the value below which 10% of the observations may be found, P50 and P90. In the present study, this modelling is performed using the exploratory modelling tool GeoX[1]

[1] A decision support software for risk, resource and economic evaluation of exploration projects, provided by Schlumberger Ltd. (https://www.software.slb.com/products/geox).

which also allows to calculate the distribution of metal content in deposits given the number of undiscovered accumulations. This distribution gives an overview of what might be discovered from individual deposits depending on the number of unknown occurrences stipulated being present in the permissive tracts.

## 5. Results

### 5.1. Grades and tonnages

Variations in grades and tonnages are reported for SMS and VMS deposits (Table 2 and 3), and respective grade-and -tonnage cumulative frequency curves (Fig.2 and 3) were computed using GeoX. Note that uncertainty resides in every aspect of SMS deposits since they are generally not well-explored, nor mined. Because surface samples do not represent the bulk composition of an entire SMS deposit, and since little is known about the interior of their potential orebodies (e.g., distribution of commodities and deposit geometry), the grade-tonnage characteristics of seafloor occurrences are not comparable with those of land-based analogues. Nevertheless, large differences would exist if the tonnage-grade characteristics of SMS deposits were representative of their potential orebodies. Grade data are shown to be higher in SMS deposits, especially when mineralization is triggered in ultramafic-hosted environments (e.g., medians of 4.82 and 16.01 wt.% of Cu in mafic- and ultramafic-related deposits, respectively) and compared to their ancient analogues (2 wt.% of Cu). Similar comparisons can be implied for other commodities (Table 2; Fig.3) which allow the recognition of possibly important gaps in resource potential between VMS and SMS deposits. Additional statistics on the size of land-based occurrences (Table 3) evidence important mineral potential (0.765 Mt as median), but large deviations (4.13 Mt). The median is close to that estimated by Mosier et al. (2009) for all types of VMS deposits (i.e., 0.71 Mt). However, it differs by one order of magnitude with tonnages currently estimated for worldwide seabed deposits (0.07 as median; Hannington et al., 2010) (Fig.2), which may be due to (1) the compiling of VMS deposits, usually reported with sufficient size to be mined, and (2) the size of seabed ore deposits considered, which is generally a function of spreading rate, a peculiarity not discriminated by Hannington et al. (2010) in their median estimate, nor in Mosier's model of VMS tonnages.

### 5.2. Metal endowment

The results of the evaluation process are separate probabilistic estimates provided for Cu, Zn, Ag and Au, and total amount of metal. Detailed quantitative analyses applied to each commodity can be seen in Table 4 and visualized on

Fig.4. Given all commodities taken together, about 447,000 tonnes of metals are estimated possibly found in-place on average if permissive tracts of volcanic zones were explored altogether. Other assumed unknown accumulations dispersed within the entire ridge valley floor increase the metal quantity on average up to 618,000 tonnes. Copper and zinc are predicted to be the major component of the potential mineral resource in terms of quantity (325,000 and 121,000 tonnes, or 72% and 27% of the total metal resource, respectively). Gold and silver provide additional resources for less than 1% of total metals estimated (about 9.12 and 231 tonnes, respectively).

### 5.3. Deposit size distribution

The size-by-rank diagram of metal accumulations (Fig.5) presents the expected amount of metals accumulated for a given number of undiscovered deposits potentially present in the permissive tracts. Results show that the largest and smallest accumulations have mean resources of 139,000 and 1,190 tonnes respectively. Most of the accumulations appear to equilibrate between 20,000 and 5,000 tonnes of metals on average, while a portion of them (~12-13%) are measured to contain lower (< 5,000 tonnes) or higher (> 20,000 tonnes) metal content toward the maximum and minimum limits of accumulation numbers respectively. These values are comparable to the metal potential of some large seabed sulfide deposits evaluated (e.g., the TAG sulfide mound and stockwork with at least 30 thousand tonnes of metals; Hannington et al., 1998), but these generally have accumulated over large areas for thousands of years (Lalou et al., 1995; Cherkashov et al., 2016).

## 6. Discussion

### 6.1. Resource abundance

Compared to global mine production (e.g., in 2017; USGS, 2018), the contained metals estimated on the Mohns Ridge are relatively minor, i.e. Cu is about 1.6% (given ~20 Mt of annual production), Zn is ~0.9% (13 Mt), Ag is 0.9% (25 kt) and Au is 0.3% (3 kt). However, estimates are expressed in probabilistic form to overcome the uncertainty specified for the unknown characteristics of SMS orebodies. Thereby, it cannot be excluded that few large deposits concentrate most of metal content (0.985 Mt in the upper confidence limit; Table 4) as illustrated in the ranked size distribution (Fig.5). The source of variation is also inherently dependent on grades attributed to each commodity, but the coefficient of variation of metal grades for VMS (e.g., 56% for Cu) is not as contrasted as that for seafloor surface samples (76%; Table 2), which makes regional endowments comparatively less uncertain with

VMS as it could be with SMS data. Furthermore, the median concentrations reported (i.e., 2 and 0.7 wt% of Cu and Zn, and 0.5 and 12 ppm of Au and Ag) are quite consistent with the average bulk composition calculated for the drilled TAG mound-stockwork complex (i.e., 2.83 and 0.42 wt% of Cu and Zn, and 0.53 and 14 ppm of Au and Ag; Hannington et al., 1998), but even subtle changes (hundred ppm) of grade values in our distributions (Fig.3) have important impact on the total endowments calculated. For this reason, if SMS orebodies are proved to consist of higher average metal contents than terrestrial mines, as presaged from surface samples at the seafloor, then the contained base and precious metals and related gross metal values calculated for undiscovered deposits (in Table 4) may eventually be conservative estimates.

As previously assumed, additional mineral resources may lie in older crust of the ridge valley and are expected to increase mineral potential (+28% in base and precious metals). However, these undiscovered resources are likely to be buried under a sediment or lava carapace in areas recognized not being affected by disrupting structures and generally close to the ridge flanks (Juliani and Ellefmo, 2018). Additional mineralization conducted by disseminations, veinlets, layers or pods transgressing within sedimentary bedding or volcanic lavas may raise the possibility for buried orebodies from either side of the ridge axis. Including these undetermined grounds into the resource assessment is not exempt from bias though because no observable imprints of geological processes allow to recognize what rock type exists at and below the seafloor. Furthermore, it is conceivable that easily accessible terrains, i.e. at outcropping structures, and perhaps within the first few meters-depth of basement, make up prospective zones for economic ore deposits. In general, repeated investigations by conventional methods such as shipboard bathymetric and oceanographic surveys, and visual observation are required prior to the discovery of hydrothermal fields, while more deeply buried deposits are more difficult to locate and require sensitive analytical techniques (e.g., self-potential method, magnetic and gravity surveying; Tivey and Johnson, 2002; Kinsey et al., 2008; Kawada and Kasaya, 2017) or in-situ drilling (e.g., Zierenberg et al., 1998) to make deeper underground examination.

In addition to the above-mentioned buried deposits, note that the permissive geology considered for the estimates in this study excludes regions beyond the ridge valley. Yet, there is now ample evidence of fossil and active hydrothermal deposits in these regions from recent seafloor surveys within both mafic- and ultramafic-hosted environments (e.g., Bach et al., 2002; Cherkachev et al., 2013; Wheeler et al., 2013), notably at the Mohns Ridge

(Pedersen et al., 2010). Since the seafloor was once formed at the median ridge axis, SMS deposits likely generated during that time and then drifted off-axis during oceanic spreading. Furthermore, the off-axis tectonic regions possibly consist of stable fault systems allowing long-lasting fluid flows to generate massive accumulations of sulfides over large time spans (McCaig et al., 2007). Thereby, the resource potential of the Mohns Ridge is probably much higher than estimated from this study.

## 6.2. Uncertainties

### 6.2.1. Tonnage

As for any estimate, theoretical models can yield alternative results depending on the assessment method and dataset used. In this study, a closed-form of quantitative assessment is adjusted with VMS deposits, but a major source of uncertainty is tonnage (Fig.2) (Hannington et al., 2010). Current inventories of SMS evidences, despite having generally higher grades, are typically reported with tonnages (e.g., ranging from <1 to above 10 Mt; Hannington et al., 2011) smaller than some classes of VMS deposits (e.g., the bimodal-mafic Kidd Creek or the mafic-siliciclastic Windy Craggy deposits with 148 and 297 million tonnes respectively; Galley et al., 2007). Discrepancies in the characteristics of modern deposits with those from land-based equivalents point out the lack of (reliable) explorative data and knowledge on both (1) the spatial and temporal development of mineralization (deposit-scale), and (2) the post-accumulation evolution of associated deposits with tectonic processes (regional-scale). At the deposit-scale, interpretation of isolated outcrops is often a substitute solution to delineate covered mineralization. Large deposits may have footprints extending over tens to hundreds of thousands of square meters (e.g., Zenith Victory, Puy des Folles, Krasnov and Alvin Zone; Hannington et al., 2010; Cherkashev et al., 2008; 2013) and would correspondingly host significant underlying resources (up to 15 Mt estimated). However, such an approach often overestimates orebody dimensions because sulfide outcrops can be affected by e.g., sedimentation and plume fall-out, potential local mass-wasting and collapsed chimneys entrained within debris flow and subsequent deposition (e.g., Webber et al., 2015). Yet, information on the continuity and thickness of sulfide outcrops is required to make reliable estimates. Drilling, and perhaps geophysical methods (e.g., magnetics and electromagnetics) are indispensable for accurate and qualitative analyses. Examples of drilled SMS deposits, such as the Bent Hill at Middle Valley on the Juan de Fuca Ridge (Zierenberg et al., 1998), the TAG mound at the Mid-Atlantic Ridge (Hannington et al., 1998) and the Solwara 1 in the eastern Manus Basin (Lipton, 2012), presented clear manifestations of relatively massive mineralization (from about 2 to 10 Mt) being assuredly of economic interest. Further transforming of drill hole into block model representation would naturally be the next steps in deciphering what is actually possible to exploit from the rocks.

### 6.2.2. Tectonic setting

Transposing the grade and tonnage models presented in this study (Tables 2 and 3; Fig.2 and 3) directly to areas of permissive geology from the modern seafloor is debatable. Indeed, the deposits considered in the models (Supplementary Tables 2 and 3), despite having similar metallogeny, may have peculiar deposit attributes and regional geologic setting that likely affected the size and metal content of ore occurrence, and to some extent, their abundance and distribution. Especially, tectonic setting of the mineral deposit may have repercussion on conditions of ore mineralizations (given e.g., spreading rate, magma type, and influence of sedimentation in ore genesis) and associated mineralogical composition of these ores. As previously said, the models from Mosier et al. (2009), which are revised in this research, refer to VMS deposits formed in extensional tectonic settings, including both oceanic seafloor spreading and arc environments. However, these deposits are generally preserved in arc-related ophiolitic complexes (Allen et al., 2002; Franklin et al., 1998) which, because much of the ancient seafloor was subducted, leave few ophiolite suites as remnants of obducted seafloor (Galley and Koski, 1999). Ophiolitic terrains thus regularly incorporate lavas with geochemical characteristics of oceanic arc or back-arc magmatism rather than mid-ocean ridge magmatism, a peculiarity attributed to their origin from supra-subduction zone (SSZ) environments (Miyashiro, 1973; Pearce et al., 1984). Based on geochemistry and field observations, both MOR and SSZ origins are often proposed and debated for the genesis of several ophiolites. Associated volcanic sections usually incorporate multiple generations of lavas that resemble either normal mid-ocean ridge basalts (N-MORB) in composition or comprise products from subduction-related magmatism depicting various tectonic settings (e.g., true oceanic environment, marginal basin or fore-arc environment for the Semail ophiolite; Pearce et al., 1981; Alabaster et al., 1982; Boudier et al., 1997; Searle and Cox, 1999; Shervais, 2001; Godard et al., 2006; Dilek and Furnes, 2009; Kusano et al., 2012; MacLeod et al., 2013). Related VMS deposits can be found to occur at multiple volcano-stratigraphic horizons (e.g., Hoxha et al., 2005; Gilgen et al., 2014) and, therefore, the mafic host-rock may show compositional variations with slab-derived components. To which degree subduction processes influenced the evolution of arc magmas and related metal content of VMS deposits is source of debate. Yet, sulfide ores from arc-related hydrothermal systems may appear to contain relatively higher contents of economically important metals (e.g., Cu and Au) compared to sulfides from sediment-starved hydrothermal systems along MORs (Herzig et al., 1993; Hannington et al., 2005; Jenner et al., 2010). Previous studies pointed out that degassing of magmatic volatiles (e.g., $H_2O$, $CO_2$, HCl and $SO_2$), generally richer in magmas generated in a subduction zone (Wallace, 2005; Plank et al., 2013), could be an important metal source in addition to metals normally leached from the oceanic crust, and thus significantly influence the metal content of the circulating hydrothermal fluids (Yang and Scott, 2003) as several metals (e.g., Cu, Au and Pb) preferentially partition into exsolving magmatic volatile phases (Williams-Jones and Heinrich, 2005; Simon and Ripley, 2011; Wohlgemuth-Ueberwasser et al., 2015). This direct contribution of metals may vary, however, depending on the metal's behavior during magmatic differentiation. For example, the behavior of Cu and Au is controlled by the oxidation state of sulfur (S), which has been suggested to be primarily a function of the magmatic oxygen fugacity (fO2; Jugo et al., 2005; Jugo, 2009), being itself dependent on water content and thus dehydration of the subducted slab. These metals act as incompatible elements when sulfate ($SO_4$(2-)) is the dominant sulfur species appearing during oxidation but become strongly compatible with the onset of sulfide saturation, i.e. after converting S6+ to S2− due to sulfate reduction (Sun et al., 2013, 2015; Liang et al., 2009; Jenner et al., 2010). The sulfate reduction can be triggered by subsequent magnetite crystallization (i.e., $Fe_3O_4$; Jenner et al., 2010; 2012; 2015) and leads to a loss of Cu and Au during magma differentiation. Metal behavior during magmatic differentiation thus ultimately controls the metal budget available for hydrothermal alteration in the sheeted dike complex or the exsolved vapor fluids. However, this tendency is variable from basin to basin depending on magma evolution and depth of magma chamber (Li et al., 2016).

Taken together, the uncertainties related to the geodynamic setting of ophiolites and the deposit characteristics (e.g., major sulfide minerals, stockwork zone and host-rock type), as well as their related preservation given by e.g., regional metamorphisms and deformations, have yet unclear direct relationships with metal content of VMS deposits, and thus, this complicates our perception on how the presence or absence of the characteristics of both ore deposits and related ophiolitic environment affect the grades and tonnages. Nevertheless, on-land analogues have geological similarities to modern deep-sea environments, and a cautious approach would essentially be to treat analogue data, such as those used in this study (Supplementary Tables 2 and 3), as close as possible to observations in modern settings.

#### 6.2.3. Modification processes

It is conceivable for analogue mineral deposits to exhibit slightly divergent ore characteristics (i.e., at least on bulk composition, mineralogy, and deposit shape and size) since the majority of ancient VMS deposits have been affected by regional metamorphism and deformation (Mosier et al., 2009; Dusel-Bacon, 2012), and possibly, former seafloor hydrothermal and weathering modifications that tend to obscure primary ore features (e.g., Herzig et al., 1991; Prichard and Maliotis, 1998). Within the ocean crust of spreading axes, high-temperature seawater-derived fluids (from 200 to above 350°C; German and von Damm, 2004) circulate and give rise to high-grade metamorphism (up to amphibolite facies), and discharge to black-smoker type vents (e.g., Liou and Ernst, 1979). After spreading, the off-axis oceanic crust that hosts SMS deposits may be subject to low-temperature (< 100°C) hydrothermal activity (Lister, 1982) which results in forming lower-grade metamorphic products (down to zeolite facies; Liou & Ernst, 1979). Associated alteration products, from axial to off-axis zones, are typically indicated from secondary minerals that associate specific phases, e.g. argillic minerals, zeolites, carbonates, epidotes, amphiboles (e.g., Schiffman et al., 1987; Alt, 1995). Within the first kilometers from the ridge axis, highly oxidizing conditions and high water-rock ratio (≥50) prevail within the upper lava pile (Gillis and Robinson, 1988). Such open circulation of seawater through the upper crust can persist for over 65 Ma as heat is extracted from the axial ridge to off-axis ridge flank crust (Stein and Stein, 1994). As spreading continues, the older oceanic lithosphere progressively cools and becomes closed to circulation systems given that related pore spaces clog with secondary hydrothermal alteration products (Davis and Elderfield, 2004) and sedimentary cover isolates the basaltic crust from seawater (Stein and Stein, 1994), making the hydrothermal regime to drive at much lower water-rock ratio.

To which degree metals have been mobilized during these hydrothermal processes is questionable. Especially, gold enrichment by later low-temperature hydrothermal activity has been evidenced to take place at off-axis regions (20-30 km from axis) within silicified umbers (Prichard and Maliotis, 1998). The Au-bearing silicifying fluids may cross-cut fossilized SMS deposits (or impregnate other lithologies) and trigger a second phase of Au mineralization that post-dates SMS deposition. As observed in a number of the ophiolitic VMS deposits (and associated sediments), gold content can be significant (e.g., from the Troodos ophiolite; Mosier et al., 1983; Hannington et al., 1998; Herzig et al., 1991; Prichard and Maliotis, 1998). Mobilization of this element may have occurred in zones of pervasive oxidative hydrothermal weathering that can extend down to the umber-lava interface or even into the 10 to 300 m deep extrusive section (Roberton & Xenophontos, 1993; Gillis, 1987; Gillis & Robinson, 1990). Seafloor weathering also forms submarine gossans and these are commonly Au-rich (Herzig et al., 1991; Galley and Koski, 1999). Similar gossans are evidenced in sub-aerial environments where oxidation and supergene enrichment proceed (Koski, 2010). Supergene enrichment results from reactions between ore and gangue minerals with meteoric waters that lead to mobilization of metals from the massive ore to depths where they are re-precipitated (Koski, 2010). Residual materials remain in the form of an altered and leached Fe oxide-rich gossan capping the underlying, less altered, primary ore. Gossans may have concentration of native gold, and a variety of silver minerals, that are of economic interest in VMS deposits because Au-bearing arsenopyrite and pyrite grains rapidly dissolve (Boyle, 1996). Underneath the cap, secondary sulfates mainly compose an oxidized zone, below which an enrichment zone developed abundant chalcocite and other Cu-rich sulfides (Koski, 2010).

Regional metamorphism and deformation are additional processes affecting the primary ore texture of VMS deposits (e.g., Vokes, 1971, 1976; Laznicka, 1985; Cook et al., 1994; Cartwright and Oliver, 2000; Marshall et al., 2000; Marshall and Gilligan, 1993; Zheng et al., 2013). As summarized by Marshall et al. (1998), well-documented (prograde) changes induced by metamorphism can (economically) upgrade or downgrade ore grades depending on the mineralogical changes. Such modifications can be e.g. (1) an increase of the FeS content of sphalerite, thereby decreasing the Zn content in recovery (downgrade; Sangster and Scott, 1976), (2) an exsolution of ZnS from chalcopyrite which makes sphalerite abundance increase, and enhances Cu content for recovery (upgrade; Sangster and Scott, 1976); re-equilibration of sphalerite with other sulfide minerals can proceed below 300°C (Aftabi et al., 2006), and (3) a release and portioning of gold from pyrite, increasing its availability (together with Ag; Larocque et al., 1995). These metamorphic changes may thus have significant impacts on the recovery of economic metals. Selective removal of metals from the ore mass during metamorphism could ultimately modify the consistency of orebody compositions, but this remains to be quantified.

Later eroded, orogenic belts containing VMS deposits also expose a variety of deformed rocks with textural changes indicating redistribution of components, sometimes upgrading the metal budget of the mineral deposit (e.g., Larocque et al., 1995; Glen et al., 1995). As described by Marshall et al. (1998), both mechanical and fluid-associated advective processes operate to produce secondary ore textures (and structures) that result in brittle deformation, ductile deformation, and annealing. Deformation dismembers and rearranges the internal elements of a deposit, and externally remobilizes components into long seams of metal-bearing rocks that can be profitable to extract. Diffusive and advective mass transfer at relatively low-temperature and high strain conditions may effectively upgrade (internal) ores by grain size coarsening and formation of discrete trace elements mineral. Alternatively, brittle deformation and shearing can produce cataclastic textures in which sulfides ingress by dislocation flow during micro-fracturing. Resulting ore components can be locally (and externally) remobilized into extensional veins, dilational jogs, and piercement structures filled by chalcopyrite and pyrrhotite. Related relocation of phase minerals may end up in a veinlet system of pyrite-chalcopyrite. However, advanced folding and thrusting involving gross displacement of ore components can dismember the deposit and thus downgrade it. Further imbrications and duplexing of displaced materials can result in structural thickening and internal ore complications that may require additional cost for recovery. The consequences of related remobilizations can thus be beneficial or disadvantageous, essentially in terms of recovery. Nevertheless, to what degree remobilization and metamorphic processes affect ore grades remains uncertain.

**Conclusion**

A number of observations about VMS deposits (grades and sizes) have allowed us to demonstrate the likelihood of recoverable resources for some deposits along the Mohns Ridge. About 447,000 tonnes of metals are inferred to reside within the volcanically active areas and it should be noted that statistical (and geological) uncertainties are included in this quantification, notably those related to the estimation model and style. Such results could be compared with other ridge-to-ridge resource estimates, and for that matter, higher resolution bathymetry would help delineating more accurately permissive tracts and certainly deciphering, with complementary observational data, typical environments for deposits that are already established e.g., in sedimentary or more tectonic regions. Despite the general enthusiasm for deep-sea mining, as a new emerging industry, there is a varying level of uncertainty about SMS orebodies (average grade, total ore tonnage and geometry) that needs to be addressed by drilling if future companies aim to establish mining activities, and perhaps, adjust current mineral deposit models for in-house assessment procedures. Even under the most optimistic circumstances of successful explorations, it is noteworthy that the in-situ metal estimates presented here may or may not be of economic value, and it is also the responsibility of engineers to provide sustainable solutions whose costs must be compared with resource estimates, as is normal practice in the oil and gas industry.

**Acknowledgements**

We wish to thank our colleague Stephen John Lippard for providing us with valuable comments and corrections of the early manuscript draft. This work was supported by the Norwegian University of Science and Technology (NTNU). Two anonymous reviewers improved the quality of the manuscript with valuable comments and suggestions and are gratefully acknowledged.

**References**

Adamides, N., 2010. Mafic-dominated volcanogenic sulphide deposits in the Troodos ophiolite, Cyprus Part 2 - A review of genetic models and guides for exploration. Applied Earth Science: Transactions of the Institutions of Mining and Metallurgy, Section B 119: 193-204.

Adamides, N.G., 1980. The form and environment of formation of the Kalavasos ore deposits - Cyprus; In: Panayiotou, A. (ed.), Ophiolites; Proc. Int. Ophiolite Symp., 1979, Cyprus Geol. Surv. Dept., pp. 117-128.

Aftabi, A., Ghodrati, Z., MacLean, W.H., 2006. Metamorphic textures and geochemistry of the Cyprus-type massive sulfide lenses at Zurabad, Khoy, Iran. J. Asian Earth Sci. 27: 523-533.

Alabaster, T., Pearce, J.A., Malpas, J., 1982. The volcanic stratigraphy and petrogenesis of the Oman ophiolite complex. Contrib. Mineral. Petrol. 81: 168-183.

Alabaster, T., Pearce, J.A., Mallick, D.I.J., Elboushi, I.M., 1980. The volcanic stratigraphy and location of massive sulphide deposits in the Oman ophiolite. Proceedings of the International Ophiolite Symposium, Cyprus 1979: 751-757.

Allen, R.L., Weihed, P., and Global VMS Research Project Team, 2002. Global comparisons of volcanic-associated massive sulphide districts, in Blundell, D.J., Neubauer, F., and Von Quadt, A., eds., The Timing and Location of Major Ore Deposits in an Evolving Orogen: Geological Society of London Special Publication 204: 13-37.

Alt, J.C., 1995. Subseafloor processes in mid-ocean ridge hydrothermal systems. Seafloor Hydrothermal Systems: Physical, Chemical, Biological, and Geological Interactions, pp. 85-114.

Bach W., Banerjee N.R., Dick H.J.B., and Baker E.T., 2002. Discovery of ancient and active hydrothermal systems along the ultra-slow spreading Southwest Indian Ridge 10°–16°E. Geochem. Geophys. Geosyst. 3(7), 1044.

Barrie, C.T., Hannington, M.D., 1999. Classification of volcanic-associated massive sulfide deposits based on host-rock composition. Rev. Econ. Geol. 8:1-11.

Beaulieu, S.E., Baker, E.T., German, C.R., and Maffei, A., 2013. An authoritative global database for active submarine hydrothermal vent fields. Geochem. Geophy. Geosy. 14: 4892-4905.

Beccaluva, L., Coltorti, M., Prempti, I., Saccani, E., Siena, F., Zeda, O., 1994. Mid-ocean ridge and supra-subduction affinities in ophiolitic belts from Albania. Ofioliti 19: 77-96.

Bel'tenev, V.E., Lazareva, L.I., Cherkashev, G.A., Ivanov, V.I., Rozhdestvenskaya, I.I., Kuznetsov, V.A., Laiba, A.A., Narkevskiy, E.V., 2017. New hydrothermal sulfide fields of the Mid-Atlantic Ridge: Yubileinoe (20°09′ N) and Surprise (20°45.4′ N). Doklady Earth Sciences 476(1): 1010-1015.

Bogdanov, Y.A., Sagalevich, A.N., Chernyaev, E.S., Gurvich, E.G., Lukashin, V.N., Ivanov, G.V., Peresypkin, V.I., 1995. Hydrothermal field at 14°45’N Mid-Atlantic Ridge. Doklady Ross. Akad. Nauk, 365(5).

Bortolotti, V., Kodra, A., Marroni, M., Mustafa, F., Pandolfi, L., Principi, G., Saccani, E., 1996. Geology and petrology of the ophiolitic sequences in the Mirdita region, northern Albania. Ofioliti 21: 3-20.

Boudier, F., Nicolas, A., Ildefonse, B., Jousselin, D., 1997. EPR microplates, a model for the Oman ophiolite. Terra Nova 9: 79-82.

Boudier, F., Ceuleneer, G., Nicolas, A., 1988. Shear zones, thrusts and related magmatism in the Oman ophiolite: initiation of thrusting on an oceanic ridge. Tectonophysics 151: 275-296.

Boyle, D.R., 1996. Supergene base metals and precious metals, in Eckstrand, O.R., Sinclair, W.D., and Thorpe, R.I., eds., Geology of Canadian mineral deposit types: Geologic Survey of Canada, Geology of Canada no. 8; Geological Society of America, Decade of North American Geology, P1, pp. 92-108.

Bruvoll, V., Breivik, A.J., Mjelde, R., Pedersen, R.B., 2009. Burial of the Mohn-Knipovich seafloor spreading ridge by the Bear Island Fan: Time constraints on tectonic evolution from seismic stratigraphy. Tectonics 28: TC4001.

Çakir, Ü., 1995. Geological characteristics of the Aşiköy-Toykondu (Küre-Kastamonu) massive sulfide deposits. Mineral. Res. Expl. Bull., 117, Ankara, pp. 29-40.

Cartwright, I., Oliver, N.H.S., 2000. Metamorphic fluids and their relationship to the formation of metamorphosed and metamorphogenic ore deposits. In: Metamorphosed and Metamorphogenic
Ore Deposits (eds Marshall B, Vokes F). Reviews in Economic Geology 11: 81–96.

Cherkashev, G.A., Ivanov, V.N., Bel'tenev, V.I., Lazareva, L.I., Rozhdestvenskaya, I.I., Samovarov, M.L., Poroshina, I.M., Sergeev, M.B., Stepanova, T.V., Dobretsova, I.G., Kuznetsov, V.Y., 2013. Massive sulfide ores of the northern equatorial Mid-Atlantic Ridge. Oceanology, 53:607-619.

Cherkashov, G., Poroshina, I., Stepanova, T., Ivanov, V., Bel'tenev, V., Lazareva, L., Rozhdestvenskaya, I., Samovarov, M., Shilov, V., Glasby, G., 2010. Seafloor massive sulfides from the northern equatorial Mid-Atlantic Ridge: new discoveries and perspectives. Mar. Georesour. Geotechnol. 28: 222-239.

Cherkashov, G., Bel'tenev, V., Ivanov, V., Lazareva, L., Samovarov, M., Shilov, V., Stepanova, T., Glasby, G.P., Kuznetsov, V., 2008. Two New Hydrothermal Fields at the Mid-Atlantic Ridge. Mar. Georesources Geotechnol. 26: 308-316.

Cherkashov, G., Kuznetsov, V., Kuksa, K., Tabuns, E., Maksimov, F., Bel'tenev, V., 2016. Sulfide geochronology along the Northern Equatorial Mid-Atlantic Ridge. Ore Geology Review 87: 147-154.

Cook, N., Klemd, R., Okrusch, M., 1994. Sulphide mineralogy, metamorphism and deformation in the Matchless massive sulphide deposit, Namibia. Mineralium Deposita 29: 1-15.

Cox, D.P., Singer, D.A., 1986. Mineral deposit models: U.S. Geological Survey Bulletin 1693: 318-348.

Da Cruz, M.I.F.S., 2015. Mineralogy and Geochemistry of contrasting hydrothermal systems on the Arctic Mid Ocean Ridge (AMOR): The Jan Mayen and Loki's Castle vent fields. Ph.D. thesis, Universidade de Lisboa, Faculdade de Ciencias.

Dauteuil, O., Brun, J.P., 1996. Deformation partitioning in a slow spreading ridge undergoing oblique extension: Mohns Ridge, Norwegian Sea. Tectonics 15: 870-884.

Davis, E., and Elderfield, H., 2004. Hydrology of the oceanic lithosphere. Cambridge University Press. London.

Dilek, Y., and Furnes, H., 2009. Structure and geochemistry of Tethyan ophiolites and their petrogenesis in subduction rollback systems. Lithos. 113: 1-20.

Dilek, Y., Eddy, C.A., 1992. The Troodos (Cyprus) and Kizildag (S. Turkey) ophiolites as structural models for slow-spreading ridge segments. Journal of Geology 100: 305-322.

Duckworth, R.C., Knott, R., Fallick, A.E., Rickard, D., Murton, B.J., Van Dover, C.L., 1995. Mineralogy and sulphur isotope geochemistry of the Broken Spur sulphides, 29°N, Mid-Atlantic Ridge. In: Parson LM, Walker CL, Dixon DR (eds) Hydrothermal vents and processes. Geological Society, London, Spec. Pub. Geol. Soc. Lond. 87: 175-189.

Dusel-Bacon, C., 2012. Petrology of metamorphic rocks associated with volcanogenic massive sulfide deposits in volcanogenic massive sulfide occurrence model: U.S. Geological Survey Scientific Investigations Report 2010–5070 –C, chap. 17, 10.

Ernewein, M., Pflumo, C., Whitechurch, H., 1988. The death of an accretion zone as evidenced by the magmatic history of the Sumail ophiolite (Oman). Tectonophysics 151: 247-274.

European Commission, 2015. Report on critical raw materials for the EU (https://ec.europa.eu/docsroom/documents/10010/attachments/1/translations/en/renditions/pdf).

Fouquet, Y., Cambon, P., Etoubleau, J., Charlou, J.L., Ondreas, H., Barriga, F.J.A.S., Cherkashov, G., Semkova T., Poroshina, I., Bohn, M., Donval, J.P., Henry, K., Murphy, P., Rouxel, O., 2010. Geodiversity of hydrothermal processes Along the Mid-Atlantic Ridge and Ultramafic-Hosted Mineralization: A New Type of Oceanic Cu-Zn-Co-Au Volcanogenic Massive Sulfide Deposit. Article in Geophysical Monograph Series 188: 321-367.

Fouquet, Y., Wafik, A., Cambon, P., Mevel, C., Meyer, G., Gente, P., 1993. Tectonic setting and mineralogical and geochemical zonation in the Snake Pit sulfide deposit (Mid-Atlantic Ridge at 23° N). Econ. Geol. 88(8): 2014-2032.

Franklin, J.M., Gibson, H.L., Jonasson, I.R., Galley, A.G., 2005. Volcanogenic massive sulfide deposits. In: Hedenquist, J.W., Thompson, J.F.H., Goldfarb, R.J., and Richards, J.P., eds, Economic Geology One Hundredth Anniversary Volume: Society of Economic Geologists, pp. 523-560.

Franklin, J.M., Hannington, M.D., Jonasson, I.R., and Barrie, C.T., 1998. Arc-related volcanogenic massive sulphide deposits: Proceedings of Short Course on Metallogeny of Volcanic Arcs, January 24-25, Vancouver: British Columbia Geological Survey Open-File 1998-8, N1-N32.

Franklin, J.M., Lydon, J.W., Sangster, D.F., 1981. Volcanic-associated massive sulfide deposits. Econ. Geol. 75: 485-627.

Galley, A.G., Hannington, M., Jonasson, I., 2007. Volcanogenic massive sulphide deposits. In: Goodfellow WD, ed., Mineral deposits of Canada - A synthesis of major deposit-types, district metallogeny, the evolution of geological provinces, and exploration methods. Geological Association of Canada, Mineral Deposits Division, Special Publication 5: 141-161.

Galley, A.G., Koski, R.A., 1999. Setting and characteristics of ophiolite-hosted volcanogenic massive sulfide deposits. In: Barrie, C.T., and Hannington, M.D., Volcanic-associated massive sulfide deposits-Processes and examples in modern and ancient settings. Reviews in Economic Geology 8: 221-246.

Gass, I.G., Lippard, S.J., Shelton, A.W., Boyle, J.F., Robertson, A.H.F., 1984. in Ophiolites and Oceanic Lithosphere, Evolving metallogenesis at the Troodos spreading axis, Geological Society, London, Special Publication, eds Gass, I.G., Lippard, S.J., Shelton, A.W., 13: 169-181.

Géli, L., Renard, V., Rommevaux, C., 1994. Ocean crust formation processes at very slow spreading centers: A model for the Mohns Ridge, near 72°N, based on magnetic, gravity, and seismic data. Journal of Geoph. Res. 99: 2995-3013.

German, C., Petersen, S., Hannington, M.D., 2016. Hydrothermal exploration of mid-ocean ridges: where might the largest sulfide deposits occur? Chem. Geol. 420:114-126.

German, C.R., and Von Damm, K.L., 2004. Hydrothermal processes. In: Holland, H.D., Turekian, K.K. and Elderfield, H. (eds.) Treatise on geochemistry, Vol. 6. The oceans and marine geochemistry. Oxford, UK, Elsevier-Pergamon, pp. 181-222.

Gilgen, S.A., Diamond, L.W., Mercolli, I., Al-Tobi, K., Maidment, D.W., Close, R., Al-Towaya, A., 2014. Volcano-stratigraphic Controls on the Occurrence of Massive Sulfide Deposits in the Semail Ophiolite. Oman. Econ. Geol. 109: 1585-1610.

Gillis, K.M., Robinson, P.T., 1990. Multistage alteration in the extrusive sequence of the Troodos ophiolite Malpas, J., Moores, E., Panayiotou, A., Xenophontos, C. (Eds.), Ophiolites, Oceanic Crustal Analogues. Proc. Symp. 'Troodos 1987', Cyprus Geological Survey Department, 655-664

Gillis, K.M., and Robinson, P.T., 1988. Distribution of alteration zones in the upper oceanic crust. Geology 16: 262-266.

Gillis, K.M., 1987. Multistage alteration of the extrusive sequence, Troodos ophiolite, Cyprus Ph.D. dissertation, Dalhousie Univ.

Glen, R.A., Walshe, J.L., Bouffler, M., Ho, T., and Dean, J.A., 1995. Syn- and post-tectonic mineralization in the Woodlawn deposit, New South Wales, Australia, Economic Geology 90: 1857-1864.

Goddard, M., Bosch, D., Einaudi, F., 2006. A MORB source for low-Ti magmatism in the Semail ophiolite. Chemical Geology 234: 58-78.

Hannington, M.D., Herzig, P.M., Scott, S.D., Thompson, G., Rona, P.A., 1991. Comparative mineralogy and geochemistry of gold-bearing sulfide deposits on the mid-ocean ridges. Marine Geology 101: 217-248.

Hannington, M.D., Jamieson, J., Monecke, T., Petersen, S., Beaulieu, S., 2011. The abundance of seafloor massive sulfide deposits. Geology 39(12): 1155-1158.

Hannington, M.D., Jamieson, J., Monecke, T., Petersen, S., 2010. Modern sea-floor massive sulfides and base metal resources: toward an estimate of global sea-floor massive sulfide potential. Spec. Publ. Soc. Econ. Geol. 15: 317-338.

Hannington, M.D., de Ronde, C.E.J., Petersen, S., 2005. Sea-floor tectonics and submarine hydrothermal systems, in Hedenquist, J.W., Thompson, J.F.H., Goldfarb, R.J., and Richards, J.P., eds, Economic Geology One Hundredth Anniversary Volume: Society of Economic Geologists 111-141.

Hannington, M.D., Galley, A.G., Herzig, P.M., Petersen, S., 1998. Comparison of the TAG mound and stockwork complex with Cyprus-type massive sulphide deposits, in Proceedings of the Ocean Drilling Program, Scientific Results, 158: 389-415.

Herzig, P.M., Hannington, M.D., Fouquet, Y., von Stackelberg, U., and Petersen, S., 1993. Gold-rich polymetallic sulfides from the Lau back arc and implications for the geochemistry of gold in seafloor hydrothermal systems of the Southwest Pacific. Economic Geology, 88: 2182-2209.

Herzig, P.M., Hannington, M.D., Scott, S.D., Maliotis, G., Rona, P.A., and Thompson, G., 1991. Gold-rich sea-floor gossans in the Troodos ophiolite and on the Mid-Atlantic ridge. Economic Geology and the Bulletin of the Society of Economic Geologists 86: 1747-1755.

Honnorez, J.J., Alt, J.C., Humphris, S.E., Herzig, P.M., Miller, D.J., Becker, K., Brown, D., Bruegmann, G.E., Chiba, H., Fouquet, Y., Gemmell, J.B., Guerin, G., Hannington, M.D., Holm, N.G., Iturrino, G.J., Knott, R., Ludwig, R.J., Nakamura, K-I., Petersen, S., Reysenbach, A-L., Rona, P.A., Smith, S.E., Sturz, A.A., Tivey, M.K., Zhao, X., 1998. Vivisection and autopsy of active and fossil hydrothermal alterations of basalt beneath and within the TAG hydrothermal mound, in Herzig, P.M., Humphris, S.E., Miller, D.J., Zierenberg, R.A., eds., TAG-Drilling an active hydrothermal system on a sediment-free slow-spreading ridge, site 957: Proceedings of the Ocean Drilling Program, Scientific Results, 158: 231-254.

Hoxha, L., Scott, P.W., Eyre, J.M., 2005. The geological setting of volcanogenic sulphide orebodies in Albanian ophiolites. Applied Earth Science (Trans. Inst. Min. Metall.) 114: 33-52.

Humphris, S.E., Cann, J.R., 2000. Constraints on the energy and chemical balances of the modern TAG and ancient Cyprus sea-floor sulphide deposits. J. Geophys. Res. 102: 28,477-28,488.

Humphris, S.E., Herzig, P.M., Miller, D.J., Alt, J.C., Becker, K., Brown, D., Brugmann, G., Chiba, H., Fouquet, Y., Gemmell, J.B., Guerin, G., Hannington, M.D., Holm, N.G., Honnorez, J.J., Iturrino, G.J., Knott, R., Ludwig, R., Nakamura, K., Petersen, S., Reysenbach, A.L., Rona, P.A., Smith, S., Sturz, A.A., Tivey, M.K., Zhao, X., 1995. The internal structure of an active sea-floor massive sulphide deposit. Nature 377: 713-716.

Hurst, S.D., Moores, E.M., Varga, R.J., 1994. Structural and geophysical expression of the Solea graben, Troodos Ophiolite, Cyprus. Tectonics 13: 139-156.

Hurst, S.D., Moores, E.M., Varga, R.J., 1987. Structure of the Solea Graben, Cyprus, from, gravity and paleomagnetic data. Geol. Soc. Am., Abstr. with Programs, 19.

Jenner, F.E., Hauri, E.H., Bullock, E.S., König, S., Arculus, R.J., Mavrogenes, J.A., Mikkelson, N., and Goddard, C., 2015. The competing effects of sulfide saturation versus degassing on the behavior of the chalcophile elements during the differentiation of hydrous melts. Geochemistry, Geophysics, Geosystems 16.

Jenner, F.E., Arculus, R.J., Mavrogenes, J.A., Dyriw, N.J., Nebel, O., and Hauri, E.H., 2012. Chalcophile element systematics in volcanic glasses from the northwestern Lau Basin. Geochemistry, Geophysics, Geosystems 13.

Jenner, F.E., O'Neill, H.C., Arculus, R.J., and Mavrogenes, J.A., 2010. The magnetite crisis in the evolution of arc-related magmas and the initial concentration of Au, Ag, and Cu, J. Petrol., 51(12): 2445-2464.

Jugo, P.J., 2009. Sulfur content at sulfide saturation in oxidized magmas. Geology 37(5): 415-418.

Jugo, P.J., Luth, R.W., Richards, J.P., 2005. An experimental study of the sulfur content in basaltic melts saturated with immiscible sulfide or sulfate liquids at 1300°C and 1·0 GPa. Journal of Petrology 46: 783-798.

Juliani, C., Ellefmo, S.L., 2018. Probabilistic estimates of permissive areas for undiscovered seafloor massive sulfide deposits on an Arctic Mid-Ocean Ridge. Ore Geology Reviews, 95: 917-930.

Kawada, Y., & Kasaya, T. (2017). Marine self-potential survey for exploring seafloor hydrothermal ore deposits. Scientific Reports, 7.

Kappel, E.S., Ryan, W.B.F., 1986. Volcanic episodicity and a non-steady state rift valley along the Northeast Pacific Spreading centers: Evidence from SeaMARC I. Journal of Geophysical Research, 91: 13,925-13,940.

Kinsey, J.C., Tivey, M.A., Yoerger, D.R., 2008. Toward high-spatial resolution gravity surveying of the mid-ocean ridges with autonomous underwater vehicles: Oceans 2008 Marine Technology Society-Institute of Electrical and Electronics Engineers Conference, Quebec City, Canada, 15-18, September 2008, Proceedings, 10p.

Koski, R.A., 2010. Supergene ore and gangue characteristics in volcanogenic massive sulfide occurrence model: U.S. Geological Survey Scientific Investigations Report 2010–5070 –C, 12, 6p.

Krasnov, S.G., Cherkashev, G.A., Stepanova, T.V., Batuyev, B.N., Krotov, A.G., Malin, B.V., Maslov, M.N., Markov, V.F., Poroshina, I.M., Samovarov, M.S., Ashadze, A.M., Lazareva, L.I., Ermolayev, I.K., 1995. Detailed geological studies of hydrothermal fields in the North Atlantic. In "Hydrothermal Vents and Processes" (L.M. Parson, C.L Walker and D.R Dixon, eds), 43-64. Geological Society, London. Special Publication 87.

Kusano, Y., Adachi, Y., Miyashita, S., Umino, S., 2012. Lava accretion system around mid-ocean ridges: Volcanic stratigraphy in the Wadi Fizh area, northern Oman ophiolite. Geochemistry, Geophysics, Geosystems, 13.

Lalou, C., Reyss, J.L., Brichet, E., Rona, P.A., Thompson, G., 1995. Hydrothermal activity on a $10^5$-year scale at a slow-spreading ridge, TAG hydro- thermal field, Mid-Atlantic Ridge 26°N. Journal of Geophysical Research 100: 17,855-17,862.

Larocque, A.C.L., Hodgson, C.J., Cabri, L.J., Jackman, J.A., 1995. Ion-microprobe analysis of pyrite, chalcopyrite and pyrrhotite from the Mobrun VMS deposit in northwestern Quebec: evidence for metamorphic remobilization of gold. Can. Mineral. 33: 373-388.

Laznicka, P., 1985. Precambrian Empirical Metallogeny. Vol 1. Phanerozoic Environments, Associations and deposits. 1002 pp. Elsevier.

Li, Z.W., Ni, S.D., Zhang, B.L., Bao, F., Zhan, S.Q., Deng, Y., Yuen, D.A., 2016. Shallow magma chamber under the Wudalianchi volcanic field unveiled by seismic imaging with dense array, Geophys. Res. Lett. 43.

Liang, H.Y., Sun, W.D., Su, W.C., Zartman, R.E., 2009. Porphyry copper-gold mineralization at Yulong, China, promoted by decreasing redox potential during magnetite alteration. Econ. Geol. 104 (4): 587-596.

Liou, J.G., and Ernst, W.G., 1979. Oceanic ridge metamorphism of the East Taiwan ophiolite. Contrib. Mineral. Petrol. 68: 335-348.

Lippard, S.J., Shelton, A.W., Gass, I.G., 1986. The Ophiolite of Northern Oman. Blackwell Scientific Publications, Oxford.

Lipton, I.T., 2012. Mineral resource estimate, Solwara Project, Bismarck Sea, Papua New Guinea. Technical Report compiled under NI43-101.

Lister, C.R.B., 1982. “Active” and “passive” hydrothermal systems in the oceanic crust: Predicted physical conditions. In: The dynamic environment of the ocean floor, Fanning KA, and Manheim FT, editors, Heath, Lexington, MA, pp. 441-470.

Macdonald, K.C., Fox, P.J., Alexander, R.T., Pockalny, R., Gente, P., 1996. Volcanic growth faults and the origin of Pacific abyssal hills. Nature 380: 125-129.

MacLeod, C.J., Lissenberg, C.J., Bibby, L.E., 2013. “Moist MORB” axial magmatism in the Oman ophiolite: the evidence against a mid-ocean ridge origin. Geology 41: 459-462.

Marshall, B., Vokes, F.M., Larocque, A.C.L., 2000. Regional metamorphic remobilization: upgrading and formation of ore deposits. Rev. Econ. Geol. 11: 19-38.

Marshall, B., Vokes, F.M., and Larocque, A.C.L., 1998. Regional metamorphic remobilization: upgrading and formation of ore deposits, in Vokes, F.M., Marshall, B., and Spry, P.G., Metamorphic and Metamorphogenic Ore Deposits, Soc. Of Econ. Geo., Reviews in Economic Geology 11.

Marshall, B., Gilligan, L.B., 1993. Remobilization, syn-tectonic processes and massive sulphide deposits. Ore Geology Reviews 8: 39-64.

McCaig, A.M., Cliff, R.A., Escartin, J., Fallick, A.E. and MacLeod, C.J., 2007. Oceanic detachment faults focus very large volumes of black smoker fluid. Geology, 35, 935-938.

McQueen, K.G., 1990. The Dragset copper-zinc deposit: a deformed, volcanogenic sulphide occurrence in the Løkken greenstones, Central Norway. Norsk Geologisk Tidsskrift 70: 1-19.

Miyashiro, A., 1973. The Troodos ophiolitic complex was probably formed in an island arc. Earth and Planetary Science Letters 19: 218-224.

Moores, E.M., Vine, F.J., 1971. Troodos Massif, Cyprus and other ophiolites as oceanic crust: evaluation and implications. Philos. Trans. R. Soc. London A 268: 443-466.

Mosier, D.L., Berger, V.I., Singer, D.A., 2009. Volcanogenic massive sulfide deposits of the world: Database and grade and tonnage models. Open-File Report 2009-1034, U.S. Department of the Interior/U.S. Geological Survey, 50p.

Mosier, D.L., Singer, D.A., and Salem, B.B., 1983. Geologic and grade-tonnage information on volcanic-hosted copper- zinc-lead massive sulfide deposits. U.S. Geol. Surv. Open- File Rep., pp. 83-89.

Murton, B.J., Klinkhammer, G., Becker, K., Briais, A., Edge, D., Hayward, N., Rouse, I., Rudnicki, M., Sayanagi, K., Sloan, H., Parson, L., 1994. Direct evidence for the distribution and occurrence of hydrothermal activity between 27 and 30 degrees north on the Mid-Atlantic Ridge. Earth Planet. Sci. Lett. 125: 119-128.

Nicolas, A., Boudier, F., Meshi, A., 1999. Slow spreading accretion and mantle denudation in the Mirdita ophiolite (Albania). J. Geophys. Res. 104: 15,155-15,167.

Parsons, T., Thompson, G.A., 1993. Does magmatism influence low-angle normal faulting? Geology 21:247-250.

Pearce, J.A., Lippard, S.J., Roberts, S., 1984. Characteristics and tectonic significance of supra-subduction zone ophiolites. Geological Society of London Special Publications 16: 74-94.

Pearce, J.A., Alabaster, T., Shelton, A.W., Searle, M.P., 1981. The Oman ophiolite as a cretaceous arc-basin complex: evidence and implications. Phil. Trans. R. Soc. Lond. A300, 299-317

Pedersen, R.B., Thorseth, I.H., Nygård, T.E., Lilley, M.D., Kelley, D.S., 2010. Hydrothermal activity at the Arctic mid-ocean ridges, in: Rona, P.A., Devey, C.W., Dyment, J., Murton, B.J. (Eds.), Geophysical Monograph Series. American Geophysical Union, Washington, D.C., pp. 67-89.

Pezard, P.A., Anderson, R.N., Ryan, W.B.F., Becker, K., Alt, J.C., Gente, P., 1992. Accretion, structure and hydrology of intermediate spreading-rate oceanic crust from drill hole experiments and seafloor observations. Marine Geophysical Researches 14(2): 93-123.

Plank, T., Kelley, K.A., Zimmer, M., Hauri, E.H., and Wallace, P.J., 2013. Why do mafic arc magmas contain ∼4 wt.% water on average? Earth Planet. Sci. Lett. 364: 168-179.

Prichard, H.M., and Maliotis, G., 1998. Gold mineralization associated with low-temperature, off-axis, fluid activity in the Troodos ophiolite, Cyprus. Journal of the Geological Society 155: 223-231.

Robertson, A.H.F., Ionescu, C., Hoeck, V., Koller, F., Onuzi, K., Bucur, I.I., Ghega, D., 2012. Emplacement of the Jurassic Mirdita ophiolites (southern Albania): evidence from associated clastic and carbonate sediments. Int. J. Earth Sci. 101: 1535-1558.

Robertson, A., and Xenophontos, C., 1993. Development of concepts concerning the Troodos ophiolite and adjacent units in Cyprus, in Magmatic Processes and Plate Tectonics, edited by Prichard, H.M., et al. Geol. Soc. Spec. Publ. 76: 85-119.

Rona, P.A., 2005. TAG hydrothermal field: A key to modern and ancient seafloor hydrothermal VMS ore-forming systems, in: Mineral Deposit Research, Meeting the Global Challenge: Proceedings of the Eighth Biennial SGA Meeting Beijing, China, 18–21 August 2005, 687-690.

Rona, P.A., Hannington, M.D., Raman, C.V., Thompson, G., Tivey, M.K., Humphris, S.E., Lalou, C., Petersen, S., 1993. Active and relict sea-floor hydrothermal mineralization at the TAG hydrothermal field, Mid-Atlantic Ridge. Econ. Geo. 88: 1989-2017.

Sangster, D., Scott, S.D., 1976. Precambrian strata-bound massive Cu-Zn-Pb sulfide ores of North America, in Wolf, K.H., ed., Handbook of strata-bound and stratiform ore deposits. Amsterdam, Elsevier, pp. 129-222.

Savannah Resources Plc, 2014. Savannah Expands into the Highly Prospective Oman Copper Belt. Available online at: https://www.rns-pdf.londonstockexchange.com/rns/5510E_-2014-4-10.pdf

Schiffman, P., Bettison, L., and Smith, B., 1987. Mineralogy and geochemistry of epidosites from the Solea graben, Troodos ophiolite, Cyprus. Ophiolites: Oceanic Crustal Analogues: Proceedings of the Symposium Troodos, 673-683.

Searle, M.P., Cox, J., 1999. Tectonic setting, origin, and obduction of the Oman ophiolite. Geol. Soc. Am. Bull. 111(1): 104-122.

Shervais, J.W., 2001. Birth, death, and resurrection: The life cycle of supra-subduction zone ophiolites: Geochemistry, Geophysics, Geosystems, 2.

Shallo, M., 1994. Outline of the Albanian ophiolites. In: Beccaluva L (ed) Albanian ophiolites-state of the art and perspectives. Spec Iss Ofioliti 19: 57-75.

Shallo, M., 1991. Ophiolitic mélange and flyschoidal sediment of the Tithonian–Lower Cretaceous in Albania. Terra Nova 2: 476-483.

Simon, A.C., and Ripley, E.M., 2011. The role of magmatic sulfur in the formation of ore deposits: Reviews in Mineralogy and Geochemistry 73: 513-578.

Singer, D.A., Kouda, R., 2011. Probabilistic estimates of number of undiscovered deposits and their total tonnages in permissive tracts using deposit densities. Nat. Resour. Res. 20: 89-93.

Singer, D.A., Menzie, W.D., 2010. Quantitative mineral resource assessments, an integrated approach. Oxford University Press.

Singer, D.A., 1993. Basic concepts in three-part quantitative assessments of undiscovered mineral resources. Non-Renewable Resources 2(2): 69-81.

Stein, C.A., and Stein, S., 1994. Constraints on hydrothermal heat flux through the oceanic lithosphere from global heat flow. J. Geophys. Res. 99: 3081-3096.

Stern, R.J., 2004. Subduction initiation: Spontaneous and induced. Earth Planet. Sci. Lett. 226: 275-292.

Sun, W., Huang, R.F., Li, H., Hu, Y.B., Zhang, C.C., Sun, S.J., Ling, M.X., 2015. Porphyry deposits and oxidized magmas. Ore Geol. Rev. 65: 97-131.

Sun, W.D., Liang, H.Y., Ling, M.X., Zhan, M.Z., Ding, X., Zhang, H., Yang, X.Y., Li, Y.L., Ireland, T.R., Wei, Q.R., Fan, W.M., 2013. The link between reduced porphyry copper deposits and oxidized magmas. Geochim. Cosmochim. Acta 103: 263-275.

Tivey, M.A., Johnson, H.P., 2002. Crustal magnetization reveals subsurface structure of Juan de Fuca Ridge hydrothermal vent fields. Geology 30: 979-982.

Tremblay, A., Meshi, A., Bédard, J.H., 2009. Oceanic core complexes and ancient oceanic lithosphere: Insights from Iapetan and Tethyan ophiolites (Canada and Albania). Tectonophysics 473: 36-52.

U.S. Geological Survey, 2018. Mineral commodity summaries 2018: U.S. Geological Survey, 200p. https://doi.org/10.3133/70194932.

Varga, R.J., Gee, J.S., Bettison-Varga, L., Anderson, R.S., Johnson, C.L., 1999. Early establishment of seafloor hydrothermal systems during structural extension: paleomagnetic evidence from the Troodos ophiolite, Cyprus. Earth Planet. Sci. Lett. 171: 221-235.

Vogt, P.R., 1986. The present plate boundary configuration, in: Vogt, P.R., Tucholke, B.E. (eds.), The Geology of North America, Volume M: The Western North Atlantic Region. Geological Society of America, Boulder, CO, 189-204.

Vokes, F.M., 1976. A review of the base metal deposits of the Norwegian Caledonides. In: Wolf KH (Editor), Handbook of strata-bound and stratiform ore deposits, 6, Elsevier, Amsterdam, The Netherlands 79-128.

Vokes, F.M., 1971. Some aspects of the regional metamorphic mobilization of pre-existing sulphide deposits. Mineralium Deposita 6: 122-129.

Wallace, P.J., 2005. Volatiles in subduction zone magmas; concentrations and fluxes based on melt inclusion and volcanic gas data. Journal of Volcanology and Geothermal Research 140: 217-240.

Warren, C.J., Parrish, R.R., Waters, D.J., Searle, M.P., 2005. Dating the geologic history of Oman's Semail ophiolite: insights from U–Pb geochronology. Contrib Mineral Petrol 150: 403-422.

Webber, A.P., Roberts, S., Murton, B.J., Hodgkinson, M.R.S., 2015. Geology, sulfide geochemistry and supercritical venting at the Beebe Hydrothermal Vent Field, Cayman Trough. Geochem. Geophys. Geosyst. 16: 2661-2678.

Whattam, S.A., and Stern, R.J., 2011. The 'subduction-initiation rule': A key for linking ophiolites, intra-oceanic forearcs and subduction initiation: Contributions to Mineralogy and Petrology, 162: 1031-1045.

Wheeler, A.J., Murton, B., Copley, J., Lim, A., Carlsson, J., Collins, P., Dorschel, B., Green, D., Judge, M., Nye, V., Benzie, J., Antoniacomi, A., Coughlan, M., Morris, K., 2013. Moytirra: Discovery of the first known deep-sea hydrothermal vent field on the slow-spreading Mid-Atlantic Ridge north of the Azores. Geochem. Geophys. Geosystems, 14.

Williams-Jones, A.E., Heinrich, C.A., 2005. Vapor transport of metals and the formation of magmatic hydrothermal ore deposits. Economic Geology 100: 1287-1312.

Wohlgemuth-Ueberwasser, C.C., Viljoen, F., Petersen, S., Vorster, C., 2015. Distribution and solubility limits of trace elements in hydrothermal black smoker sulfides: An in-situ LA-ICP-MS study. Geochim. Cosmochim. Acta 159: 16-41.

Yang, K., and Scott, S.D., 2003. Geochemical relations of felsic magmas to ore metals in massive sulfide deposits of the Bathurst Mining Camp, Iberian Pyrite Belt, Hokuroku District and the Abitibi belt, Econ. Geol. Monogr. 11: 457-478.

Yigit, O., 2009. Mineral deposits of Turkey in relation to Tethyan Metallogeny: Implications for future mineral exploration. Economic Geology 104(1): 19-51.

Yildirim, N., Dönmez, C., Kang, J., Lee, I., Pirajno, F., Yildirim, E., Günay, K., Seo, J.H., Farquhar, J., Chang, S.W., 2016. A magnetite-rich Cyprus-type VMS deposit in Ortaklar: A unique VMS style in the Tethyan metallogenic belt, Gaziantep, Turkey. Ore Geology Reviews 79: 425-442.

Zheng, Y., Zhang, L., Chen, Y.J., Hollings, P., Chen, H.Y., 2013. Metamorphosed Pb–Zn–(Ag) ores of the Keketale VMS deposit, NW China: Evidence from ore textures, fluid inclusions, geochronology and pyrite compositions. Ore Geology Reviews 54: 167-180.

Zierenberg, R.A., Fouquet, Y., Miller, D.J., and Shipboard Party, 1998. The deep structure of a seafloor hydrothermal deposit. Nature 392: 485-488.

**Table 1.** Estimated number of SMS deposits on the Mohns Ridge. Values are rounded-off to the upper limit (see Juliani and Ellefmo (2018) for calculation details and delimitation of areas).

| | At neo-volcanic terrains | Within the ridge valley floor |
|---|---|---|
| **Area** (km2) | 2,922 | 5,065 |
| **Mode** | 4 | 6 |
| **Mean** | 11 | 15 |
| **Std. Dev.** | 9 | 12 |
| **Coef. Var.** | 0.81 | 0.80 |
| **F100** | 1 | 1 |
| **F95** | 2 | 3 |
| **F90** | 3 | 4 |
| **F75** | 5 | 7 |
| **F50** | 8 | 11 |
| **F25** | 14 | 19 |
| **F10** | 23 | 31 |
| **F5** | 30 | 40 |
| **F0** | 66 | 87 |

**Table 2.** Statistical summary of grade data for VMS and modern seafloor deposits (see Supplementary Tables 1 and 2 for source data.). CV is coefficient of variation, and n is the number of samples.

| **Deposit (host-rock type)** | | **Cu (wt.%)** | **Zn (wt.%)** | **Au (ppm)** | **Ag (ppm)** |
|---|---|---|---|---|---|
| SMS (mafic) | | *n=20* | *n=20* | *n=20* | *n=20* |
| | Median | 4.82 | 2.30 | 0.75 | 27 |
| | Average | 4.98 | 3.46 | 1.81 | 37.74 |
| | Min | 0.55 | 0.18 | 0.13 | 4.29 |
| | Max | 16.20 | 16.70 | 10.90 | 115 |
| | CV[1] | 76 | 121 | 144 | 88 |
| SMS (ultramafic) | | *n=8* | *n=8* | *n=8* | *n=8* |
| | Median | 16.01 | 9.45 | 7.03 | 70.5 |
| | Average | 15.10 | 10.37 | 8.63 | 74.61 |
| | Min | 2.48 | 0.83 | 3.50 | 7.80 |
| | Max | 23.40 | 25.40 | 23.80 | 188 |
| | CV | 45 | 90 | 78 | 74 |
| VMS (mafic) | | *n=59* | *n=21* | *n=13* | *n=17* |

| | | | | |
|---|---|---|---|---|
| Median | 2.00 | 0.70 | 0.50 | 12 |
| Average | 1.94 | 0.88 | 0.70 | 16.64 |
| Min | 0.24 | 0.1 | 0.1 | 0.6 |
| Max | 5 | 2.5 | 2.2 | 69 |
| CV | 56 | 74 | 77 | 97 |

**Table 3.** Statistical summary of tonnage data for VMS deposits (see Supplementary Table 3 for source data).

| | **Tonnage (Mt)** |
|---|---|
| | *n = 39* |
| Median | 0.765 |
| Average | 2.54 |
| Std.Dev. | 4.13 |
| Min | 0.02 |
| Max | 16 |

**Table 4.** Estimated contained base metals (in million tons) and precious metals (in tons) from undiscovered deposits on the Mohns Ridge.

| | **At neo-volcanic terrains** (2,922 km2) | | | | | **Within the ridge valley floor** (5,065 km2) | | | | |
|---|---|---|---|---|---|---|---|---|---|---|
| **Commodity** | Cu | Zn | Au | Ag | Total | Cu | Zn | Au | Ag | Total |
| **Mean** | 0.325 | 0.121 | 9.12 | 231 | 0.447 | 0.449 | 0.168 | 12.6 | 319 | 0.618 |
| **Std. Dev.** | 0.32 | 0.121 | 9.2 | 240 | 0.436 | 0.409 | 0.155 | 11.8 | 302 | 0.558 |
| **F90** | 0.052 | 0.019 | 1.36 | 33 | 0.073 | 0.078 | 0.028 | 2.1 | 50 | 0.11 |
| **F50** | 0.228 | 0.083 | 6.26 | 153 | 0.315 | 0.333 | 0.123 | 9.2 | 228 | 0.46 |
| **F10** | 0.718 | 0.269 | 20.51 | 521 | 0.985 | 0.969 | 0.366 | 27.6 | 702 | 1.33 |

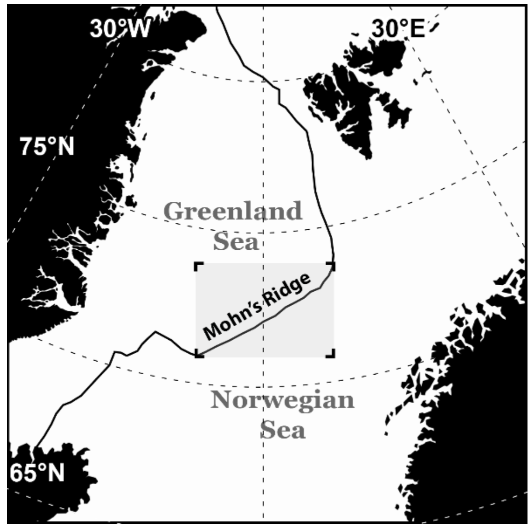


**Fig. 1** Location of the study area. A total of 510 km of rift valley floors are analyzed along the ridge trend.

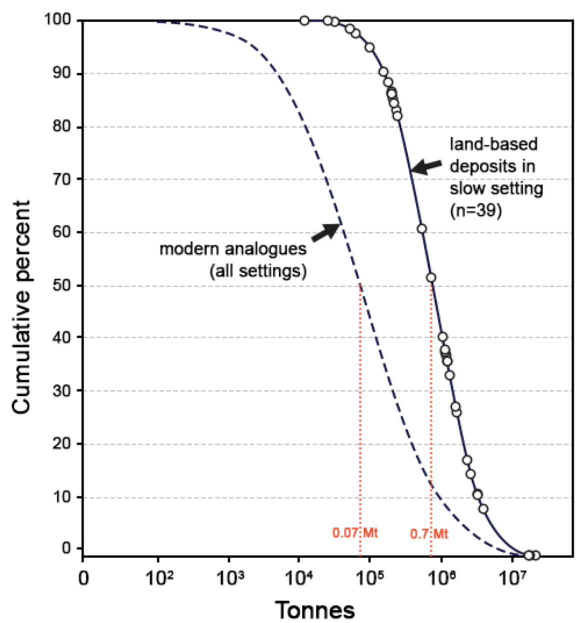


**Fig. 2** Cumulative frequency plots of tonnages for mafic-hosted VMS deposits (slow-spreading setting; this study) and SMS occurrences (all settings; Hannington et al., 2010). Original tonnage data (open circles) are plotted on respective curves. Data source from Supplementary Table 3.

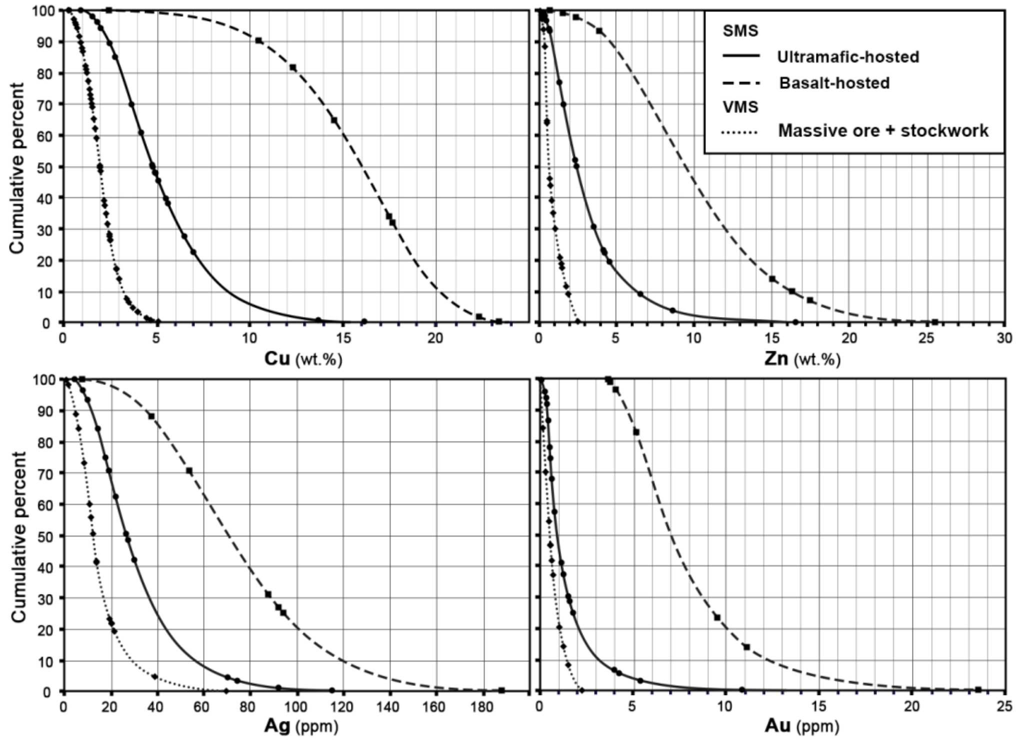


**Fig. 3** Grade and tonnage cumulative curves for VMS and SMS deposits hosted in mafic and ultramafic environments. Original grade data (black dots) are plotted on respective curves. Data source from Supplementary Tables 1 and 2.

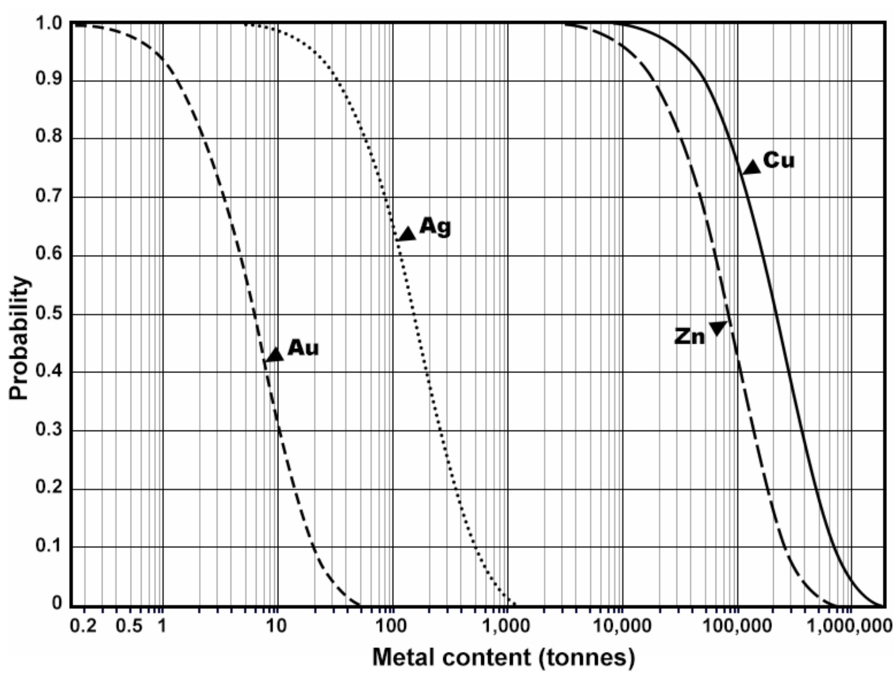


**Fig. 4** Cumulative distributions of copper (Cu), zinc (Zn), gold (Au) and silver (Ag) contained within undiscovered seafloor massive sulfide deposits of neo-volcanic zones along the Mohn's Ridge valley.

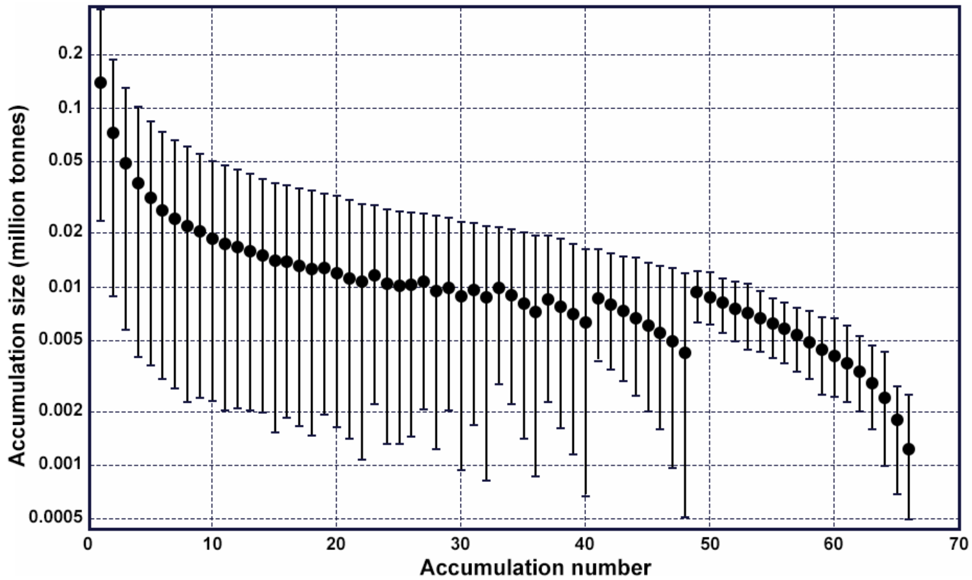


**Fig. 5** Size distribution of total undiscovered metal accumulations based on the ranked size distribution of accumulations stipulated being present in the permissive tracts. Black circles are mean values while vertical bars represent their respective 90% confidence interval (i.e., between the 10th and 90th percentiles).

**Resource Assessment of Undiscovered Seafloor Massive Sulfide Deposits on an Arctic Mid-Ocean Ridge: Application of grade and tonnage models**

Cyril Juliani, Steinar Løve Ellefmo

Norwegian University of Science and Technology (NTNU), Department of Geoscience and Petroleum, Sem Sælandsvei 1, 7491, Trondheim, Norway

Corresponding e-mails: *cyril.juliani@ntnu.no*, *steinar.ellefmo@ntnu.no*

**Table 1.** Bulk chemical composition of SMS deposits. Data given for TAG, Alvin Zone, Mir Zone, Snake Pit, Broken Spur, Krasnov, Mt Jourdanne, MAR, 24 30'N, Turtle Pits, Nibelungen: Hannington et al. (2010); Zenith Victory, Puy des Folles, Peterburgskoye, Ashadze-1, Ashadze-2, Irinovskoye, Semyenov: Cherkashov et al. (2010); Cherkashov et al. (2013); Beebe: Webber et al. (2015); Red Lion, Comfortless Cove, 49°39'E: German et al. (2016); Loki's Castle: Da Cruz (2015); Yubileinoe: Bel'tenev et al. (2017); Lucky Strike, Menez Gwen, Rainbow: Fouquet et al. (2010); Logachev-1: Bogdanov et al. (1995). Empty cells are undetermined values.

| Deposit, host-rock | Deposit (details) | # of samples | Cu (wt.%) | Zn (wt.%) | Au (ppm) | Ag (ppm) |
|---|---|---|---|---|---|---|
| SMS, mafic | TAG (surface & core) | 310 | 4.9 | 6.5 | 1.8 | 92 |
| | Alvin Zone | 7 | 2 | 0.3 | 0.85 | 17 |
| | Mir Zone | 137 | 5 | 8.7 | 4.2 | 115 |
| | Snake Pit | 93 | 6.5 | 4.6 | 1.66 | 70 |
| | Broken Spur | 76 | 4.9 | 3.7 | 1.64 | 30 |
| | Krasnov (extinct) | 137 | 5.6 | 0.4 | 1.11 | 22 |
| | Zenith Victory | 17 | 3.69 | 0.38 | 0.26 | 27.1 |
| | Puy des Folles | 19 | 13.07 | 2.41 | 0.23 | 27.5 |
| | Peterburgskoye (extinct) | 16 | 4.17 | 0.18 | 0.55 | 14.5 |
| | Beebe – Piccard | 16 | 4.81 | 0.79 | 10.9 | |
| | Mt. Jourdanne | 9 | 1.9 | 16.7 | 1.2 | 4.29 |
| | Red Lion | | 2.9 | | 0.64 | |
| | MAR, 24 30'N | | 16.2 | 4.1 | 5.3 | |
| | Loki's Castle | | 0.56 | 1.31 | 0.3 | 9.04 |
| | 49°39'E | | 1.9 | | 4 | |
| | Yubileinoe | | 4.82 | 0.74 | 0.49 | 19.2 |

| | | | | | | |
|---|---|---|---|---|---|---|
| | Lucky Strike (hot spot) | 154 | 5.37 | 4.16 | 0.3 | 74 |
| | Turtle Pits (boiling) | 43 | 7 | 2.3 | 0.26 | 17 |
| | Menez Gwen (boiling) | 26 | 1.75 | 1.66 | 0.13 | 27 |
| | Confortless Cove (boiling) | | 2.5 | | 0.42 | |
| SMS, ultramafic | Ashadze-1 | 97 | 10.52 | 17.64 | 3.5 | 87.7 |
| | Ashadze-2 | 51 | 17.7 | 0.83 | 11.1 | 7.8 |
| | Logachev-1 | 78 | 23.4 | 3.9 | 8.95 | 37 |
| | Logachev-2 | 5 | 14.72 | 25.4 | 23.8 | 92 |
| | Nibelungen | 9 | 17.3 | 16.2 | 8.95 | 37 |
| | Irinovskoye | 25 | 22.24 | 1.58 | 4.07 | 94.1 |
| | Rainbow | 116 | 12.43 | 14.99 | 5.1 | 188 |
| | Semyenov | 63 | 2.48 | 2.39 | 3.6 | 53.3 |

## References to Table 1


Bel'tenev, V.E., Lazareva, L.I., Cherkashev, G.A., Ivanov, V.I., Rozhdestvenskaya, I.I., Kuznetsov, V.A., Laiba, A.A., Narkevskiy, E.V., 2017. New hydrothermal sulfide fields of the Mid-Atlantic Ridge: Yubileinoe (20°09′ N) and Surprise (20°45.4′ N). Doklady Earth Sciences 476(1): 1010-1015.

Bogdanov, Y.A., Sagalevich, A.N., Chernyaev, E.S., Gurvich, E.G., Lukashin, V.N., Ivanov, G.V., Peresypkin, V.I., 1995. Hydrothermal field at 14°45’N Mid-Atlantic Ridge. Doklady Ross. Akad. Nauk, 365(5).

Da Cruz, M.I.F.S., 2015. Mineralogy and Geochemistry of contrasting hydrothermal systems on the Arctic Mid Ocean Ridge (AMOR): The Jan Mayen and Loki's Castle vent fields. Ph.D. thesis, Universidade de Lisboa, Faculdade de Ciencias.

Cherkashev, G.A., Ivanov, V.N., Bel'tenev, V.I., Lazareva, L.I., Rozhdestvenskaya, I.I., Samovarov, M.L., Poroshina, I.M., Sergeev, M.B., Stepanova, T.V., Dobretsova, I.G., Kuznetsov, V.Y., 2013. Massive sulfide ores of the northern equatorial Mid-Atlantic Ridge. Oceanology, 53:607-619.

Cherkashov, G., Poroshina, I., Stepanova, T., Ivanov, V., Bel'tenev, V., Lazareva, L., Rozhdestvenskaya, I., Samovarov, M., Shilov, V., Glasby, G., 2010. Seafloor massive sulfides from the northern equatorial Mid-Atlantic Ridge: new discoveries and perspectives. Mar. Georesour. Geotechnol. 28: 222-239.

Fouquet, Y., Cambon, P., Etoubleau, J., Charlou, J.L., Ondreas, H., Barriga, F.J.A.S., Cherkashov, G., Semkova T., Poroshina, I., Bohn, M., Donval, J.P., Henry, K., Murphy, P., Rouxel, O., 2010. Geodiversity of hydrothermal processes Along the Mid-Atlantic Ridge and Ultramafic-Hosted Mineralization: A New Type of Oceanic Cu-Zn-Co-Au Volcanogenic Massive Sulfide Deposit. Article in Geophysical Monograph Series 188: 321-367.

German, C., Petersen, S., Hannington, M.D., 2016. Hydrothermal exploration of mid-ocean ridges: where might the largest sulfide deposits occur? Chem. Geol. 420:114-126.

Hannington, M.D., Jamieson, J., Monecke, T., Petersen, S., 2010. Modern sea-floor massive sulfides and base metal resources: toward an estimate of global sea-floor massive sulfide potential. Spec. Publ. Soc. Econ. Geol. 15: 317-338.

Webber, A.P., Roberts, S., Murton, B.J., Hodgkinson, M.R.S., 2015. Geology, sulfide geochemistry and supercritical venting at the Beebe Hydrothermal Vent Field, Cayman Trough. Geochem. Geophys. Geosyst. 16: 2661-2678.

**Resource Assessment of Undiscovered Seafloor Massive Sulfide Deposits on an Arctic Mid-Ocean Ridge: Application of grade and tonnage models**

Cyril Juliani, Steinar Løve Ellefmo

Norwegian University of Science and Technology (NTNU), Department of Geoscience and Petroleum, Sem Sælandsvei 1, 7491, Trondheim, Norway

Corresponding e-mails: cyril.juliani@ntnu.no, steinar.ellefmo@ntnu.no

**Table 2.** Bulk chemical composition of selected Cyprus-type VMS deposits. Data given for Norway: McQueen (1990); Mosier et al. (2009); Albania: Hoxha et al. (2005); Mosier et al. (2009); Turkey: Çakir (1995); Yigit (2009); Yildirim et al. (2016); Oman: Savannah Resources Plc. (2014); Mosier et al. (2009); others: Mosier et al. (2009). Empty cells are undetermined values.

| Country | Deposit | Cu (wt.%) | Zn (wt.%) | Au (ppm) | Ag (ppm) |
|---|---|---|---|---|---|
| Albania | Rubiku | 2.01 | 0.7 | 0.5 | |
| | Palai-Karme | 2.48 | 0.9 | 0.4 | |
| | Porave | 2.15 | 1.4 | | |
| | Derven | 0.98 | 0.24 | | |
| | Rehova | 1.86 | 0.5 | 0.6 | 20 |
| | Kachinar | 3.85 | 1.55 | 0.5 | 12 |
| | W Kachinar | 1.45 | 0.8 | 0.5 | 12 |
| *Turkey* | Ortaklar | 2.32 | 0.32 | 0.735 | 5.365 |
| | Toykondu | 4 | | 1.55 | |
| | Anayatak (Ergani) | 1.39 | | | |
| | Mihrapdag (Ergani) | 2.5 | | 1.2 | |
| | Siirt Madenkoy | 1.55 | | | |
| | Kure (Asikoy) | 2.17 | | 2.2 | 11 |
| | Kure (Bakibaba) | 2.2 | | 1 | |
| Colombia | Sababablanca | 5 | | | |
| Canada | Chu Chua | 2 | 0.4 | 0.44 | 8.66 |
| | Sunro | 1.23 | | 0.144 | 1.45 |
| | Huntingdon | 0.9 | | 0.1 | 0.6 |

| | | | | | |
|---|---|---|---|---|---|
| Cuba | Cacarajicara | 1.2 | | | |
| | Jucaro | 1.38 | | | |
| Cyprus | Limni | 1.4 | | | |
| | Kokkinoyia | 1.5 | 0.2 | | |
| | Ambelikou | 1 | | | |
| | Apliki | 1.8 | | | |
| | Kapedhes | 0.5 | | | |
| | Kokkinopezoula | 0.5 | | | |
| | Kynousa | 2.04 | 1.7 | | |
| | Mavri Sykia-Landaria | 2 | | | |
| | Mousoulos-Kalavasos | 1 | 0.5 | 1.7 | 6.1 |
| | Peravasa | 0.76 | | | |
| | Petra | 2 | | | |
| | Platies | 2 | | | |
| | Sha | 0.6 | | | |
| | Agrokipia | 1.7 | 1.09 | | |
| | Troulli | 1 | | | |
| | Skouriotissa | 2.35 | 0.5 | | 69 |
| | Mathiati North | 0.24 | 0.1 | | |
| | Mavrovouni | 4 | 0.5 | 0.3 | 39 |
| Guatemala | Oxec | 3 | | | |
| Norway | Lokken | 2.1 | 1.9 | 0.3 | 19 |
| | Dragset | 2 | 2.5 | | 20 |
| Oman | Bayda | 2 | | | |
| | Lasail | 2 | | | |
| | Aarja | 2 | | | |
| | Carawison | 2.8 | | | |
| | Hatta (main) | 3.41 | | 0.3 | |

| | | | | | |
|---|---|---|---|---|---|
| | Shinas | 2 | | | |
| Philippines | Carmel | 1.48 | | | |
| | Bongbongan | 1.18 | | | |
| | Lorraine | 4.5 | | | |
| Russia | Osennee | 4.69 | 0.24 | 0.3 | 20.8 |
| | Letnee | 3.3 | 1.55 | 0.6 | 13.7 |
| | Bama | 0.55 | | | |
| | Fornas | 1.33 | | | |
| | Arinteiro | 0.9 | | | |
| Sweden | Viscaria | 1.1 | | | |
| United States | Threeman-Standard Copper | 1.08 | | 0.72 | 10.5 |
| | Rua Cove | 1.1 | | | |
| | Western World | 2.81 | 0.95 | 0.69 | 13.7 |

## References to Table 2


Çakir, Ü., 1995. Geological characteristics of the Aşiköy-Toykondu (Küre-Kastamonu) massive sulfide deposits. Mineral. Res. Expl. Bull., 117, Ankara, pp. 29-40.

Hoxha, L., Scott, P.W., Eyre, J.M., 2005. The geological setting of volcanogenic sulphide orebodies in Albanian ophiolites. Applied Earth Science (Trans. Inst. Min. Metall.) 114: 33-52.

McQueen, K.G., 1990. The Dragset copper-zinc deposit: a deformed, volcanogenic sulphide occurrence in the Løkken greenstones, Central Norway. Norsk Geologisk Tidsskrift 70: 1-19.

Mosier, D.L., Berger, V.I., Singer, D.A., 2009. Volcanogenic massive sulfide deposits of the world: Database and grade and tonnage models. Open-File Report 2009-1034, U.S. Department of the Interior/U.S. Geological Survey, 50p.

Savannah Resources Plc, 2014. Savannah Expands into the Highly Prospective Oman Copper Belt. Available online at: https://www.rns-pdf.londonstockexchange.com/rns/5510E_-2014-4-10.pdf

Yigit, O., 2009. Mineral deposits of Turkey in relation to Tethyan Metallogeny: Implications for future mineral exploration. Economic Geology 104(1): 19-51.

Yildirim, N., Dönmez, C., Kang, J., Lee, I., Pirajno, F., Yildirim, E., Günay, K., Seo, J.H., Farquhar, J., Chang, S.W., 2016. A magnetite-rich Cyprus-type VMS deposit in Ortaklar: A unique VMS style in the Tethyan metallogenic belt, Gaziantep, Turkey. Ore Geology Reviews 79: 425-442.

**Resource Assessment of Undiscovered Seafloor Massive Sulfide Deposits on an Arctic Mid-Ocean Ridge: Application of grade and tonnage models**

Cyril Juliani, Steinar Løve Ellefmo

Norwegian University of Science and Technology (NTNU), Department of Geoscience and Petroleum, Sem Sælandsvei 1, 7491, Trondheim, Norway

Corresponding e-mails: *cyril.juliani@ntnu.no*, *steinar.ellefmo@ntnu.no*

**Table 3.** Size of ophiolitic VMS deposits formed within a slow-spreading setting. Data given for Troodos: Mosier et al. (1986); Hannington et al. (1998); Adamides (2010); Mirdita: Hoxha et al. (2005).

| Ophiolite | Deposit | Tonnage (Mt) |
|---|---|---|
| Troodos | Agrokipia A | 0.765 |
| | Agrokipia B | 4.5 |
| | Alestos | 0.1 |
| | Ambelikou | 0.016 |
| | Apliki | 1.65 |
| | East lefka | 1.2 |
| | Kalavassos | 6 |
| | Kambia | 1.5 |
| | Kapedhes | 0.05 |
| | Klirou East | 0.42 |
| | Klirou West | 0.077 |
| | Kokkinopezoula | 3.5 |
| | Kokkinoyia | 0.5 |
| | Kynousa | 0.3 |
| | Kynousa Uncle Charles | 0.22 |
| | Limni | 16 |
| | Mangaleni | 0.1 |
| | Mathiatis | 2.8 |
| | Mavri Sykia | 0.376 |

| | | |
|---|---|---|
| | Mavrovouni | 15 |
| | Memi | 1.5 |
| | Mousoulos | 1.66 |
| | Peravasa | 0.09 |
| | Peristerka | 0.33 |
| | Petra | 0.526 |
| | Phoenix | 15 |
| | Phoukasa | 6 |
| | Pitharokhoma | 1.4 |
| | Platies | 0.045 |
| | Sha | 0.35 |
| | Skouriotissa | 5.44 |
| | Troulli | 0.27 |
| Mirdita (west) | Rubiku | 1.5 |
| | Palai-Karme | 2 |
| | Porave | 0.3 |
| | Derven | 1.6 |
| | Rehova | 5 |
| | Kachinar | 0.3 |
| | W Kachinar | 0.3 |

## References to Table 3

Adamides, N., 2010. Mafic-dominated volcanogenic sulphide deposits in the Troodos ophiolite, Cyprus Part 2 - A review of genetic models and guides for exploration. Applied Earth Science: Transactions of the Institutions of Mining and Metallurgy, Section B 119: 193-204.

Hannington, M.D., Galley, A.G., Herzig, P.M., Petersen, S., 1998. Comparison of the TAG mound and stockwork complex with Cyprus-type massive sulphide deposits, in Proceedings of the Ocean Drilling Program, Scientific Results, 158: 389-415.

Hoxha, L., Scott, P.W., Eyre, J.M., 2005. The geological setting of volcanogenic sulphide orebodies in Albanian ophiolites. Applied Earth Science (Trans. Inst. Min. Metall.) 114: 33-52.

Mosier, D.L., Singer, D.A., and Salem, B.B., 1986. Geologic and grade-tonnage information on volcanic-hosted copper-zinc-lead massive sulfide deposits. U.S. Geological Survey Open-File Report 83-89, 78 p.